Discrimination and Identification of Quantum States

by

Ulrike Futschik

A dissertation submitted to the Graduate Faculty in Physics in partial fulfillment of the requirements for the degree of Doctor of Philosophy, The City University of New York

2010

This manuscript has been read and accepted for the
Graduate Faculty in Physics in satisfaction of the
dissertation requirement for the degree of Doctor of Philosophy

Date	Professor Jànos A. Bergou Chair of Examining Committee
Date	Professor Steven Greenbaum Executive Officer

Professor Ying-Chih Chen _____

Professor Mark Hillery _____

Professor Edgar Feldman _____

Professor Igor Jex _____

Supervisory Committee

THE CITY UNIVERSITY OF NEW YORK

Abstract

Discrimination and Identification of Quantum States

by

Ulrike Futschik

Advisor: Professor János A. Bergou

Determining the state of a quantum system is an essential step in quantum information processing. While the case of $N = 2$ arbitrary states is well known the extension to $N > 2$ is highly non-trivial.

Unambiguous discrimination among $N > 2$ pure states is one of the longest standing unsolved problems in quantum information. We develop a complete geometric picture that encompasses all aspects of the problem: linear independence of the states, positivity of the detection operators, and a graphic method for finding and classifying the optimal solutions. We illustrate it on the example of three states and also show that the problem depends on an invariant combination of the phases of the complex inner products, the Berry phase. For arbitrary inner products and prior probabilities only numerical solutions are possible but the features of the solution are universal, they hold for any value of the Berry phase up to $\phi = \pi$ at which point it greatly simplifies. We, therefore, present the complete analytical solution for the case of vanishing Berry phase. The corresponding optimal failure probability exhibits full permutational symmetry for a large range of the parameters. However, when the parameters have very different

values, a second-order symmetry-breaking phase transition takes place: at a particular value of the parameters the optimal failure probability becomes bi-valued: a second, less symmetric solution branches away in a continuous way from the symmetric one which is optimal in the new regime for some set of parameters. We also study some special cases where the inner products of two or all three states coincide but the phase is arbitrary as well as the case of weighted equal probability measurement. The optimum measurement is derived and it is a general measurement (POVM). The generalization of our results to the discrimination of more than three states will discussed in the conclusion.

Finally, we address the problem of identifying one probe qudit with one out of N reference qudits. Two strategies, the unambiguous and the minimum error identification, are studied. The reference states are assumed to be pure states and no classical knowledge about them is available. The probe state is guaranteed to match one of the reference states with equal probability. The problem is shown to be equivalent to distinguishing between mixed quantum states. Through the example of three ququartz states the form of the optimal measurement operators is derived for the unambiguous strategy. Using the positivity constraint for the operator of the inconclusive result the optimum success probability is calculated. In the minimum error identification an upper and a lower bound are derived, the latter by using a square-root measurement. Numerical values of the success probability are calculated to which the lower bound compares favorable.

ACKNOWLEDGMENTS

I would like to express my sincere gratitude towards my advisor Prof. J. Bergou. Thank you for the many discussions and the support through ups and downs. Thank you to my committee for their time and comments in order to improve this manuscript.

Thank you to all the people I met at the Graduate Center and at Hunter College especially Bing He, Yonatan Abranyos and Istvan Nemeth for being there to talk about physics, life, the universe and everything.

Thank you to my family for always believing in me. You are always on my mind. Thank you to Jørgen for always reminding me: Don't panic!

Thank you to everyone who supported, encouraged and inspired me through these last years.

So long, and thanks for all the fish!

Contents

List of Tables

List of Figures

Chapter 1

Introduction

Quantum information processing is part of quantum information theory, a field that lies on the intersection of quantum mechanics, information theory and computer science. Its objective is to use quantum mechanical systems to process information. This very powerful idea finds practical application in the form of quantum computers and quantum cryptography.

In quantum information processing or quantum computing the information is encoded in the quantum state itself. After all desired transformation of the system are taken place this information has to be read out. Therefore the state has to be measured. However, one of the features exploited by quantum cryptography is that non-orthogonal quantum states can not be distinguished with unit probability. Hence the measurement strategy will involve some trade-off. It will be optimal in respect to a certain figure of merit. If it is important that each measurement returns a conclusive answer to what the given state of the system is, errors can not be avoided. One therefore strifes to minimize the occurrence of a wrong determination

i. e. the measurement established that state 1 was the state of the system, when it really was state 2. This strategy is known as the minimum error (ME) strategy. On the other hand if one tries to avoid ambiguity in the result the offset is that the measurement sometimes returns "I don't know" to the question to which state was given. This is called the inconclusive result. However the remaining measurements will determine the state with certainty. The optimization of this scheme consist in limiting or minimizing the inconclusive result. This strategy is known as the unambiguous state discrimination (USD).

Nielsen and Chuang [1] investigated the possibility of an equivalent in quantum computing to the universal gate array of classical computers. In this situation the set of states involved in a process is not known ahead of times. Therefore the measurement strategy has to be independent of the specific states. In order to determine which state the system is in a reference system is provided which is sometimes called the program. The unknown state called the probe or data state is guaranteed to match one of the program states. Such a measurement is referred to as state identification. While the case where the states are known is referred to as state discrimination.

For both state discrimination and state identification the above mentioned two measurement strategies can and have been employed. Though most of the analytically solved cases only involve two quantum states or high degrees of symmetry. The extension to $N > 2$ states as well as higher dimensions of the Hilbert space is far from trivial.

In this work we study the unambiguous discrimination of three non-orthogonal, pure quantum states. We show how the general structure holds

true to the extension to $N > 3$. We also investigate both unambiguous and minimum error identification of $N > 2$ qudits.

This work is structured as follows: In the remaining part of this chapter we introduce state discrimination. One of the main tools in quantum measurement, generalized measurement or POVM, is outlined briefly. Then we describe the two most widely used state discrimination strategies, minimum error discrimination and unambiguous discrimination. The last part of this chapter is concerned with state identification.

In Chapter 2 we present the unambiguous discrimination of three pure states with arbitrary complex overlaps. We start by setting up the problem and the optimal strategy. We show how the necessary condition for USD, linear independence of the states, can be quantified. Two different scalings are introduced which illuminate certain aspects of the problem. One is used to obtain a geometric interpretation of the problem and the optimum solution. The other is useful to solve the discrimination problem for real states. This is a representative case of the features for all states. Furthermore, we present the cases where the overall phase is arbitrary, but the overlap amplitudes of all states is equal or two of them are equal. Scaling in the former case allows to extend the valid parameter range of solutions. On the other hand, scaling is tantamount to weighted equal probability measurement, examples of which are shown in Section 2.5.4. Lastly, we derive the exact form of the measurement operators or POVM.

Chapter 3 starts by showing the equivalence between the identification of unknown pure states and the discrimination of mixed states. Section 3.2 treats the unambiguous identification of N unknown pure qudit states. First,

an example of three ququartz identification is given. Then we derive the general form of the detection operators. The optimum success probability is found by using positivity constraints on the detection operators. The minimum error identification of N unknown pure qudits is the subject of Section 3.3. We introduce an upper bound that is very optimistic. Then the square-root measurement is used to derive a lower bound. Numerical calculations of the optimum success probability show that the lower bound is, indeed, a very good approximation.

Finally, we conclude this work with Chapter 4 where we summarize the results.

1.1 Generalized Measurement

Distinguishing quantum states optimally requires a more general approach to measurements than the projective measurement. The positive operator valued measure (POVM) or generalized measurement describes such a measurement and will be used throughout this thesis. This treatment contains the standard Von Neumann or projective measurement as a special case. However it allows to have more measurement outcomes then the dimensionality of the system under consideration and therefore provides more flexibility.

The elements of the POVM are the positive operators Π_j with

$$\sum_j \Pi_j = I \quad and \quad \Pi_j \geq 0. \tag{1.1.1}$$

They can be expressed in terms of the detection operators A_j such that

$$\Pi_j = A_j^\dagger A_j \tag{1.1.2}$$

with $\sum A_j^\dagger A_j = I$ and $A_j = \Pi_j^{\frac{1}{2}}$. The post-measurement state is given by

$$\phi = \frac{A_j|\psi\rangle}{\langle\psi|A_j^\dagger A_j|\psi\rangle^{\frac{1}{2}}} \quad and \quad \rho_j = \frac{A_j \rho A_j^\dagger}{\mathrm{Tr}\left(A_j \rho A_j^\dagger\right)} \tag{1.1.3}$$

for pure and mixed states, respectively. Most of the time we are not interested in the state after the measurement but the probability of receiving a certain result. The probability that a measurement resulted in a particular outcome is

$$p_j = \langle\psi|\Pi_j|\psi\rangle \quad and \quad p_j = \mathrm{Tr}\left(\Pi_j \rho\right) \tag{1.1.4}$$

again for pure and mixed states, respectively. Eqs. (1.1.1) and (1.1.2) are sufficient to ensure that the probabilities p_j are positive numbers between 0 and 1 and sum to 1.

Finally, Neumark's theorem [2] states that a POVM can always be realized by extending the Hilbert space by adding an ancilla. Then the POVM is implemented as a projective measurement in this larger space.

1.2 Distinguishing Quantum States

Distinguishing quantum states is an essential task in quantum information processing. However, to differentiate between non-orthogonal states with unit probability is quantum mechanically impossible which can be seen in

the following example.

Consider two, pure states $|\psi_1\rangle$ and $|\psi_2\rangle$ which are not orthogonal to each other, $\langle\psi_1|\psi_2\rangle \neq 0$. Let us assume to the contrary of our above statement that the two detection operators Π_1 and Π_2 can indeed distinguish perfectly between the states $|\psi_1\rangle$ and $|\psi_2\rangle$. This means applying Π_1 to $|\psi_2\rangle$ or Π_2 to $|\psi_1\rangle$ should give zero, i. e.

$$\Pi_1|\psi_2\rangle = 0 \quad \text{and} \quad \Pi_2|\psi_1\rangle = 0. \tag{1.2.1}$$

On the other hand, the probabilities of correctly identifying the states $|\psi_1\rangle$ and $|\psi_2\rangle$ are

$$\langle\psi_1|\Pi_1|\psi_1\rangle = p_1 \quad \text{and} \quad \langle\psi_2|\Pi_2|\psi_2\rangle = p_2. \tag{1.2.2}$$

We reach a contradiction if we take into account the completeness relation of the detection operators

$$\Pi_1 + \Pi_2 = I. \tag{1.2.3}$$

If we apply now $\langle\psi_1|$ from the left and $|\psi_1\rangle$ from the right of Eq. (1.2.3) and the same with $\langle\psi_2|$ and $|\psi_2\rangle$ we get

$$\langle\psi_1|\Pi_1|\psi_1\rangle + \langle\psi_1|\Pi_2|\psi_1\rangle = p1 + 0 = 1 \tag{1.2.4}$$

$$\langle\psi_2|\Pi_1|\psi_2\rangle + \langle\psi_2|\Pi_2|\psi_2\rangle = 0 + p2 = 1 \tag{1.2.5}$$

and it seems we have perfect discrimination. However, if we apply $\langle\psi_1|$ from the left and $|\psi_2\rangle$ from the right of Eq. (1.2.3) and taking Eq. (1.2.1) into

account, we get

$$\langle\psi_1|\Pi_1|\psi_2\rangle + \langle\psi_1|\Pi_2|\psi_2\rangle = 0 = \langle\psi_1|\psi_2\rangle \tag{1.2.6}$$

which contradicts our assumption of non-orthogonality. Therefore, two states can only be perfectly distinguished if they are orthogonal.

Another approach then would be to try to make the states orthogonal. For example if we take the n-th tensor product of the states with themselves, $|\psi_1\rangle \otimes |\psi_1\rangle \otimes \cdots \otimes |\psi_1\rangle = |\psi_1\rangle^{\otimes n}$ and $|\psi_2\rangle \otimes |\psi_2\rangle \otimes \cdots \otimes |\psi_2\rangle = |\psi_2\rangle^{\otimes n}$, and then calculate the inner product, we get

$$\lim_{n\to\infty} \langle\psi_1|\psi_2\rangle^{\otimes n} = 0. \tag{1.2.7}$$

However, the no-cloning theorem states that we can not make a copy of an unknown quantum state [4, 5]. Hence we can not produce such states.

Consequently, state discrimination comprises finding an optimum strategy in respect to a certain figure of merit such as the requirement to always make a decision about which state is given and minimize the ambiguous results or to never make a wrong determination with the cost of gaining no information for some instances and minimizing the occurrence of such instances. The former of the two is known as minimum error discrimination and the latter as unambiguous state discrimination. They are outlined in the following sections.

Other figures of merit include the fidelity [6] and accessible information [7]. In recent years, a number of different approaches to distinguish between

quantum states have been proposed. We just list a few of them without further discussion. One, a mixed strategy, interpolates between the unambiguous discrimination and minimum error discrimination. Here, a fixed number of inconclusive results is allowed and the success probability is maximized. This strategy has been explored for both pure [8, 9, 10] and mixed states [11, 12]. Another approach, the minimax strategy [13], takes a frequentist view by abstaining to use the a priori probabilities. In this scenario the smallest of the individual success probabilities is maximized. On the other hand, discrimination with maximum confidence [14] considers to maximize all individual success probabilities. Sometimes this strategy can only be realized if an inconclusive result is permitted linking it to the unambiguous state discrimination without the requirement of linear independence. In [15] the inconclusive result for the maximum confidence strategy was minimized. Experimental implementation was demonstrated by [16, 17].

Depending on the initial knowledge about the states a distinction is drawn between state discrimination and state identification. If the task is to identify a state from a known ensemble of states $\{\psi_i\}$ with a priori probabilities η_i we talk about *state discrimination*. If the states are unknown we call it *state identification*.

1.2.1 Minimum error discrimination

There are N detection operators to discriminate between N states presented by density matrices ρ_i with $i = 1, 2, \ldots, N$. If the measurement result is i it is assumed that state ρ_i was given. If the states are not orthogonal there are erroneous outcomes, say detector j clicked but state i was given. The

averaged probability to correctly or successfully determine the state is

$$P_{corr} = \sum_{i=1}^{N} \text{Tr } \eta_i \rho_i \Pi_i \tag{1.2.8}$$

where the η_i are the a priori probabilities and the Π_i are the detection or measurement operators with $\sum_i \Pi_i = I$. The probability of making a wrong determination follows as

$$P_{err} = 1 - P_{corr} = 1 - \sum_{i=1}^{N} \text{Tr } \eta_i \rho_i \Pi_i \tag{1.2.9}$$

The task is to find a set of detection operators Π_i that minimizes errors. While necessary and sufficient conditions [18, 19, 20] for the detection operators to be optimal are known it is most of the time not possible to deduce the operators themselves from them. The conditions are

$$\Pi_k \left(\eta_k \rho_k - \eta_j \rho_j\right) \Pi_j = 0 \tag{1.2.10}$$

$$\sum_k \Pi_k \eta_k \rho_k - \eta_j \rho_j \geq 0 \tag{1.2.11}$$

The minimum of the error probability for two states was independently found by Helstrom [18] and Holevo[19]. It is given by

$$P_{err} = \frac{1}{2}\left(1 - \text{Tr}|\eta_2 \rho_2 - \eta_1 \rho_1|\right) \tag{1.2.12}$$

where $|A| = \sqrt{A^\dagger A}$ for any operator A.

We demonstrate how to derive this limit, also called the Helstrom limit, following the treatment in [21].

A quantum system is prepared in one of two possible states ρ_1 or ρ_2 with prior probabilities η_1 and η_2, respectively. The probability of making a wrong determination is given by

$$P_{err} = \eta_1 \mathrm{Tr}\left(\rho_1 \Pi_2\right) + \eta_2 \mathrm{Tr}\left(\rho_2 \Pi_1\right). \tag{1.2.13}$$

Using $\Pi_1 + \Pi_2 = I$ we can rewrite Eq. (1.2.13) in two equivlanet ways

$$P_{err} = \eta_1 + \mathrm{Tr}\left(\Lambda \Pi_1\right) = \eta_2 - \mathrm{Tr}\left(\Lambda \Pi_2\right) \tag{1.2.14}$$

where we introduced the Hermitian operator

$$\Lambda = \eta_2 \rho_2 - \eta_1 \rho_1 = \sum_{k=1}^{D_S} \lambda_k |\phi_k\rangle\langle\phi_k| \tag{1.2.15}$$

with D_S the dimensionality of the quantum system under consideration. The states $|\phi_k\rangle$ are the orthonormal eigenstates belonging to the eigenvalue λ_k. Using the spectral decomposition of Λ Eq. (1.2.14) becomes

$$P_{err} = \eta_1 + \sum_{k=1}^{D_S} \lambda_k \langle\phi_k|\Pi_2|\phi_k\rangle = \eta_2 - \sum_{k=1}^{D_S} \lambda_k \langle\phi_k|\Pi_1|\phi_k\rangle. \tag{1.2.16}$$

The task now is to find Π_1 and Π_2 such that the error probability P_{err} is minimized subject to the constraint $0 \leq \langle\phi_k|\Pi_i|\phi_k\rangle \leq 1$. It is clear that Eq. (1.2.16) reaches its minimum if $\langle\phi_k|\Pi_2|\phi_k\rangle = 1$ for states $|\phi_k\rangle$ corresponding to negative eigenvalues λ_k and $\langle\phi_k|\Pi_2|\phi_k\rangle = 0$ for states $|\phi_k\rangle$ corresponding to positive eigenvalues λ_k. On the other hand, Eq. (1.2.16) is at its minimum if $\langle\phi_k|\Pi_1|\phi_k\rangle = 0$ for states $|\phi_k\rangle$ corresponding to negative eigenvalues λ_k

and $\langle\phi_k|\Pi_2|\phi_k\rangle = 1$ for states $|\phi_k\rangle$ corresponding to positive eigenvalues λ_k. Without loss of generality we can reorder the eigenvalues λ_k in the following way

$$\lambda_k < 0 \qquad \text{for} \qquad 1 \leq k < k_0, \tag{1.2.17}$$

$$\lambda_k > 0 \qquad \text{for} \qquad k_0 \leq k \leq D, \tag{1.2.18}$$

$$\lambda_k = 0 \qquad \text{for} \qquad D < k \leq D_S. \tag{1.2.19}$$

Hence the optimum detection operators are given by

$$\Pi_1 = \sum_{k=1}^{k_0-1} |\phi_k\rangle\langle\phi_k| \quad \text{and} \quad \Pi_2 = \sum_{k=k_0}^{D} |\phi_k\rangle\langle\phi_k|, \tag{1.2.20}$$

where the eigenstates $|\phi_k\rangle$ corresponding to $\lambda_k = 0$ have to be added in such a way that $\Pi_1 + \Pi_2 = I$. These states however do not affect $P_{err}^{min} = P_E$. The error probability now is

$$P_E = \eta_1 - \sum_{k=1}^{k_0-1} |\lambda_k| = \eta_2 - \sum_{k=k_0}^{D} |\lambda_k|. \tag{1.2.21}$$

Taking the sum of these two alternative representations and using $\eta_1 + \eta_2 = 1$ we arrive at

$$P_E = \frac{1}{2}\left(1 - \sum_{k=1}^{D_S} |\lambda_k|\right) = \frac{1}{2}\left(1 - |\Lambda|\right) \tag{1.2.22}$$

which is equivalent to Eq. (1.2.12). Due to the characteristics of the detection operators in Eq. (1.2.20) we consider two cases. Suppose that there are only positive eigenvalues λ_k. Then we have $\Pi_1 = 0$ and $\Pi_2 = I$, which means that the minimum error probability P_E can be achieved by always guessing

the state was ρ_2 without measurement. Similar considerations hold true if there are only negative eigenvalues. This is in agreement with the observation [22] that measurement does not always aid minimum error discrimination. On the other hand if there are both, positive and negative eigenvalues, then the two set of eigenstates $\{|\phi_1\rangle \dots |\phi_{k_0-1}\rangle\}$ and $\{|\phi_{k_0}\rangle \dots |\phi_D\rangle\}$ span orthogonal subspaces. Therefore the measurement is a von Neumann or projective measurement. This result holds for pure and mixed states.

Unfortunately, it is in general not possible to derive the optimum POVM from the necessary and sufficient conditions Eqs. (1.2.10) and (1.2.11). However, there are some solutions for symmetric cases. The case of $N > 2$ pure qubit states was treated by Helstrom [18] and Ban *et al.* [23]. Multiply symmetric, pure states were the subject of work by Barnett [24], while the case of mirror-symmetric states was treated by Andersson *et al.* [25]. Herzog *et al.* [26] disussed the discrimination between subsets of linearly dependent state in a two-dimensional Hilbert space. The case of two non-perfectly known states was studied by Ježek [27]. The discrimination between a pure and a uniformly mixed state with application to bipartite qubit states was subject of work by Herzog [21]. The minimum error discrimination lends itself to discriminate between mixed states. The case of two mixed states was discussed by Bergou *et al* [28]. An iterative algorithm for three mixed states was presented by Ježek *et al.* [29]. Again, for more than two states solutions are only known for states which exhibit certain symmetric properties. Then either a square-root measurement [30, 31] or a semidefinite programming approach [30, 32, 33, 34] is employed. Bounds for $N > 2$ are given both for pure [35] and mixed [36, 37, 38] states.

The Helstrom bound was experimentally demonstrated by Barnett *et al.* [39]. Clarke *et al.* [40] demonstrated the experimental feasibility for the case of trine and tetrad states.

1.2.2 Unambiguous state discrimination

Consider a quantum system in state ψ_j which is one of the non-orthogonal states from the set $\{\psi_1, \psi_2, \ldots, \psi_N\}$ with $j = 1, 2, \ldots, N$. The task is to determine which state the system is in without error. This means anytime the measurement returns j we know with certainty that the state of the system was ψ_j. On the other hand because of the non-orthogonality of the states the no-error condition can only be met if we allow for one more measurement outcome, the inconclusive outcome [3]. In this case we learn nothing about which state the system was in. The measurement returns *"I don't know"* to the question which state was given. We say the procedure failed. This is called unambiguous state discrimination (USD). The concept was introduced by Ivanovic [41] to differentiate between two non-orthogonal states. Subsequently the optimal solution for two states with equal prior probability was found by Dieks [42] and Peres [43]. Jaeger and Shimony [44] extended the previous analysis to arbitrary *a priori* probabilities. A scheme for optical realization via the dual-rail representation was provided by Bergou *et al.* [45] for this case.

The no-error condition can be expressed in terms of the detection probabilities as follows

$$\langle \psi_i | A_j^\dagger A_j | \psi_i \rangle = \delta_{ij} p_i \tag{1.2.23}$$

where the $\{A_j\}$ are a set of measurement or detection operators and $i, j = 1, 2, \ldots, N$. The p_i are the individual success probabilities. Outcome j only occurs if the state was ψ_j and the probability for this is p_j. One more operator A_0 is required for the times when the procedure fails to determine the state and this occurs with probability q_i, the individual failure probability, if the state was ψ_i. The individual failure probabilities q_i are

$$\langle\psi_i|A_0^\dagger A_0|\psi_i\rangle = q_i \tag{1.2.24}$$

with

$$A_0^\dagger A_0 = I - \sum_{j=1}^{N} A_j^\dagger A_j. \tag{1.2.25}$$

This is the inconclusive or ambiguous result. No standard Von Neumann measurement can fulfill Eqs. (1.2.23) and (1.2.24). Therefore the set $\{A_j\}$ represents a generalized measurement with the POVM elements

$$\Pi_j = A_j^\dagger A_j \tag{1.2.26}$$

and $j = 0, 1, \ldots, N$.

Chefles [46], Duan *et al.* [47] and Zhang *et al.* [48] showed that the necessary and sufficient condition for unambiguous discrimination of N states is that the states are linearly independent.

Starting with a set of linearly independent states $\{\psi_i\}$ if an inconclusive result was received the states after the measurement are

$$|\phi_i\rangle \propto A_0|\psi_i\rangle. \tag{1.2.27}$$

If these post-measurement states are linearly independent, too, then we can apply another USD strategy and so on. Hence the first measurement was not optimal. Therefore a requirement for optimality is that the initially linearly independent states are mapped into linearly dependent states, the failure states. Their relationship to the individual success probabilities is

$$\langle \phi_i | \phi_j \rangle = \langle \psi_i | \psi_j \rangle - p_i \delta_{ij}. \tag{1.2.28}$$

If we consider η_i the *a priori* probabilities for each state $|\psi_i\rangle$, the total success probability for the correct determination of the states is

$$P = \sum_i \eta_i p_i \tag{1.2.29}$$

and, accordingly, the total failure probability is given by

$$Q = \sum_i \eta_i q_i. \tag{1.2.30}$$

This is the quantity we wish to minimize in the optimum discrimination strategy conditioned on the constraint that the failure states are linearly dependent.

While the formalism seems straight forward there exists no closed, analytical form for USD of $N > 2$ states. However, some special cases have been studied. Chefles [46] investigated the case of N pure non-orthogonal states. He derived the optimum measurement for N states under the constraint that the measurement outcomes are equally likely. This kind of measurement was later called the equal-probability measurement or EPM by Eldar [50].

Shortly thereafter, Chefles and Barnett [51] obtained the maximum success probability for a set of symmetric, linearly independent states with equal *a priori* probabilities. Peres and Terno [52] were the first to systematically examine the case of three non-orthogonal states providing a numerical method to find the solution and made the first attempt to introduce a geometric view of the optimization procedure. Sun *et al.* studied the case of three states when the pairwise overlaps among the states are real and at least two of them are equal in magnitude [53]. The connection of state discrimination to semidefinite programing was noticed, in the particular context of UD, by Sun [53] and Eldar *et al.* [50]. Building on this work, Jafarizadeh *et al.* [54] made further progress on the UD of three real states. Most recently, Pang and Wu [55] obtained analytical results for special cases of discriminating three states and made great advances toward developing a full geometric interpretation of the problem. Finally, in a closely related work, Roa *et al.* considered UD for N equally separated states with complex overlaps [56]. Upper and lower bounds for the case of discriminating between two mixed states were provided by Rudolph *et al.* [57]. Bergou *et al.* [28] compared the unambiguous discrimination of two mixed states to the minimum error discrimination. In addition, two mixed states are studied for special classes of density operators in [58, 59]. State filtering was discussed in [60] and [61] where it also was linked to mixed state discrimination. The discrimination of two subspaces were also presented as a case of mixed state discrimination [62]. For more than two mixed states Feng *et al.* [63] showed that for a mixed state the condition to be unambiguously discriminated from a set of states, is that its support is not completely included in the support of the

other states. A semidefinite programming approach to discriminate between mixed states was presented by Eldar *et al.* [64]

1.2.3 Identification of unknown pure states

State identification is a variant of state discrimination. The task is to identify the state ψ_j, the probe or data state, which is one of the states from the set $\{\psi_1, \psi_2, \ldots, \psi_N\}$ with $j = 1, 2, \ldots, N$. The states are unknown. In order to compensate for the lack of knowledge a set of reference states is provided also unknown. However, the probe state is guaranteed to match one of the reference or program states.

The idea to use states as programs in a quantum computer was introduced by Nielsen and Chuang [1]. The question they set out to answer was if it is possible to build a programmable quantum gate in analog to a classical universal gate array. This proved to be only possible if the gate is probabilistic. Vidal *et al.* [65] explored how to store any unitary operation in a finite number of qubits such that the operation can be retrieved later. Hillery *et al.* [66, 67, 68] extended the work to completely positive, trace perserving maps applied to qubits and qudits. Here, a program encoded in quantum states determined which operation is performed on the data state. Quantum controlled measurement devices or multimeter were discussed in Ref. [69, 70, 71]. An experimental implementation was demonstrated by Soubusta *et al.* [72].

An universal programmable quantum state discriminator that distinguishes unambiguously between two unknown states with arbitrary a priori probabilities was explored by [73]. The corresponding problem of discrimi-

nating with minimum error was treated in [74]. This was expanded to the case of two equally likely d-dimensional quantum system, qudits, for both the unambiguous [75, 76] and the minimum error strategy [76, 77]. They as well as [78, 79] also investigated the case where the reference states are each encoded in multiple copies. For unambiguous discrimination, Zhang *et al.* [80] derived the correct form of the detection operators in the case of N arbitrary states in d dimensions. A distinction between the $N = d$ case and the $N < d$ case was made. A different derivation of the detection operators was presented by Herzog and Bergou [81] for the $n_d = d$ case and the optimum success probability was given explicitly. In addition, several schemes for implementing the unambiguous identification of two unknown qubits [82, 83, 85, 84] and qudits [86] have been proposed. A scheme for measurement on composite qudits is presented by [87]. The experimental manipulation of qutrits [88] and ququarts [89] were recently demonstrated.

Chapter 2

Unambiguous Discrimination (USD) of three non-orthogonal, pure quantum states

Let us consider the Hilbert space $\mathcal{H}$ spanned by three non-orthogonal states $\{|\psi_1\rangle, |\psi_2\rangle, |\psi_3\rangle\}$. In the general case the overlaps between the states are given by:

$$\begin{aligned} \langle\psi_1|\psi_2\rangle &= s_3 e^{i\phi_{12}} \\ \langle\psi_2|\psi_3\rangle &= s_1 e^{i\phi_{23}} \\ \langle\psi_3|\psi_1\rangle &= s_2 e^{i\phi_{31}} \end{aligned} \tag{2.0.1}$$

The parameters s_i are real values from 0 to 1, and ϕ_{ij} are the phases between the states. The states are given with *a priori* probabilities η_i with $\sum \eta_i = 1$.

Let us define the combination of the phases as

$$\phi = \phi_{12} + \phi_{23} + \phi_{31}. \tag{2.0.2}$$

This is the only combination of the phases that will appear in the following treatment. It is the invariant phase of the problem, also called the geometric phase or cocycle. It corresponds to a phase deficiency associated with a closed path in parameter space ($1 \to 2 \to 3 \to 1$), therefore it is the Berry phase for the UD problem (Pancharatnam [90] and Berry [91]). If we replace the states $|\psi_j\rangle$ by equivalent states $e^{i\theta_j}|\psi_j\rangle$ we get the same Berry phase.

The parameters s_j and ϕ describe the choice of three states up to unitary equivalence. Together with the *a priori* probabilities η_i these are the parameters that define the USD problem.

2.1 Optimal USD strategy

Unambiguous state discrimination (USD) allows us to discriminate between non-orthogonal, linearly independent states without error but with the possibility of an inconclusive result. In the case of three states the POVM has four elements

$$\Pi_0 + \sum_{i=1}^{3} \Pi_i = I \quad with \quad \Pi_j \geq 0 \tag{2.1.1}$$

one each, Π_i with $i = 1, 2, 3$, to correspond to the correct determination of one of the states ψ_i and one, Π_0, for the inconclusive result with $\Pi_j = A_j^\dagger A_j$.

We wish to maximize the overall success probability

$$P = \sum_i \eta_i p_i \tag{2.1.2}$$

or, conversely, minimize the overall failure probability

$$Q = \sum_i \eta_i q_i. \tag{2.1.3}$$

where $p_i = \langle\psi_i|\Pi_i|\psi_i\rangle$ and $q_i = \langle\psi_i|\Pi_0|\psi_i\rangle$ are the individual success and failure probabilities, respectively.

The USD strategy is optimal if the initially, linearly independent states ψ_i are mapped onto linearly dependent ones, the failure states $\phi_i = A_0|\psi_i\rangle$, for the ambiguous or inconclusive outcome. We can express this condition analytically by constructing the Gram matrix of the failure states C such that the matrix elements are given by

$$C_{jk} = \langle\phi_j|\phi_k\rangle. \tag{2.1.4}$$

Explicitly we have

$$C = \begin{bmatrix} q_1 & \langle\psi_1|\psi_2\rangle & \langle\psi_1|\psi_3\rangle \\ \langle\psi_2|\psi_1\rangle & q_2 & \langle\psi_2|\psi_3\rangle \\ \langle\psi_3|\psi_1\rangle & \langle\psi_3|\psi_2\rangle & q_3 \end{bmatrix}. \tag{2.1.5}$$

The Gram matrix is always semidefinite-positive. Therefore we have

$$\det(C) \geq 0 \tag{2.1.6}$$

which leads to the following constraint

$$q_1 q_2 q_3 - q_1 s_1^2 - q_2 s_2^2 - q_3 s_3^2 + 2 s_1 s_2 s_3 \cos\phi \geq 0, \tag{2.1.7}$$

where we used Eqs. (2.0.1) and (2.0.2). The Gram matrix is strictly positive if and only if the states ϕ_j are linearly independent [92]. Hence the 'equal' sign in Eq. (2.1.7) represents linearly dependent states and therefore the optimum solution. The same constraint could be obtained by the requirement that the POVM element for the ambiguous outcome has to be positive, i. e. $\Pi_0 = I - \sum_{i=1}^{3} \Pi_i \geq 0$.

Since C is semidefinite-positive the principal minors of C are also semidefinite-positive,

$$\Delta_{kj} = q_k q_j - \langle\psi_k|\psi_j\rangle\langle\psi_j|\psi_k\rangle \geq 0, \tag{2.1.8}$$

yielding the conditions

$$\begin{aligned} \Delta_{12} &= q_1 q_2 - s_3^2 \geq 0, \\ \Delta_{13} &= q_1 q_3 - s_2^2 \geq 0, \\ \Delta_{23} &= q_2 q_3 - s_1^2 \geq 0. \end{aligned} \tag{2.1.9}$$

which will provide additional conditions for choosing the physical solution for q_i.

For the minimization of the total failure probability we take a Lagrange multiplier approach using the constraint (2.1.7)

$$Q' = \sum_i \eta_i q_i + \lambda \Delta \tag{2.1.10}$$

with Δ =det(C) and then obtain the following conditions

$$\begin{aligned}
\frac{\partial Q'}{\partial q_1} &= \eta_1 + \lambda \left(q_2 q_3 - s_1^2 \right) = 0, \\
\frac{\partial Q'}{\partial q_2} &= \eta_2 + \lambda \left(q_1 q_3 - s_2^2 \right) = 0, \\
\frac{\partial Q'}{\partial q_2} &= \eta_3 + \lambda \left(q_1 q_2 - s_3^2 \right) = 0.
\end{aligned} \tag{2.1.11}$$

If we solve these for the individual failure probabilities, we get

$$\begin{aligned}
q_1 &= \sqrt{\frac{\left(s_2^2 + \eta_2 \delta \right) \left(s_3^2 + \eta_3 \delta \right)}{\left(s_1^2 + \eta_1 \delta \right)}}, \\
q_2 &= \sqrt{\frac{\left(s_1^2 + \eta_1 \delta \right) \left(s_3^2 + \eta_3 \delta \right)}{\left(s_2^2 + \eta_2 \delta \right)}}, \\
q_3 &= \sqrt{\frac{\left(s_1^2 + \eta_1 \delta \right) \left(s_2^2 + \eta_2 \delta \right)}{\left(s_3^2 + \eta_3 \delta \right)}}
\end{aligned} \tag{2.1.12}$$

where we replaced $-\frac{1}{\lambda}$ with $\delta \geq 0$. Substituting Eqs. (2.1.12) into Eq. (2.1.7) will result in a sixth-order equation for δ which, in general, is impossible to solve analytically except for some special cases. Those cases will be discussed in Section 2.5.

2.2 Scaling properties

For some of the following it is constructive to use scaled parameters where original parameters are combined in new ways. There are several scaling properties inherent in the problem. We will just introduce two different ones that will prove useful in different settings.

The first scaling separates the parameters such that the constraint will only depend on the cocycle phase while the total average failure probability will contain the scaled overlaps but will be independent of the cocycle. But this is a less significant feature and its main use is that it helps to lend a simple geometric interpretation to the constraint.

The second scaling will reduce the number of independent parameters from seven (the three priors, the three overlaps and the cocycle phase) to four (three scaled overlap parameters and the cocycle phase). This is of advantage when we solve Eq. (2.1.12) for some special cases.

Scaling A

Let us introduce the following combination of the overlap amplitudes

$$r_1 = \frac{s_1}{s_2 s_3}, \qquad r_2 = \frac{s_2}{s_3 s_1}, \qquad r_3 = \frac{s_3}{s_1 s_2}. \tag{2.2.1}$$

With the help of these combinations we define a set of scaled failure probabilities, denoted by tilde,

$$\tilde{q}_i = r_i q_i. \tag{2.2.2}$$

In terms of these new quantities, the constraint in Eq. (2.1.7) becomes independent of the overlaps and only depends on the cocycle or Berry phase,

$$\tilde{q}_1\tilde{q}_2\tilde{q}_3 - \tilde{q}_1 - \tilde{q}_2 - \tilde{q}_3 + 2\cos\phi \geq 0 \tag{2.2.3}$$

where the equal sign stands for the optimum solution. The failure probability Q can be expressed in terms of the scaled quantities as

$$Q = \sum_{i=1}^{3} \eta_i \frac{\tilde{q}_i}{r_i}. \tag{2.2.4}$$

The positivity of the principal minors of C becomes entirely independent of the parameters,

$$\begin{aligned} \Delta_{12} &= \tilde{q}_1\tilde{q}_2 - 1 \geq 0, \\ \Delta_{13} &= \tilde{q}_1\tilde{q}_3 - 1 \geq 0, \\ \Delta_{23} &= \tilde{q}_2\tilde{q}_3 - 1 \geq 0. \end{aligned} \tag{2.2.5}$$

This scaling separates the parameters: the overlap amplitudes appear only in Eq. (2.2.4), while the cocycle phase appears only in the constraint, (2.2.3), and (2.2.5) is independent of the parameters. This scaling will be extremely useful to give a geometric view of the problem and lead to a natural classification of the solutions into three classes, described in section 2.4.

Scaling B

We introduce the scaled failure probabilities, denoted by bar

$$\bar{q}_i = \eta_i q_i, \tag{2.2.6}$$

for $i = 1, 2, 3$, then the total average failure probability can be written as

$$Q = \sum_{i=1}^{3} \bar{q}_i, \tag{2.2.7}$$

so that formally it becomes independent of the prior probabilities. Let us now recall that the overlap amplitudes were defined as $s_1 = |\langle\psi_2|\psi_3\rangle|$ in Eq.(2.0.1), and with cyclic permutations of the indexes for s_2 and s_3. We introduce the following scaling where, again, scaled quantities are denoted by bar,

$$\bar{s}_1 = \sqrt{\eta_2 \eta_3}\, s_1, \tag{2.2.8}$$

and with the obvious cyclic permutation of the indexes for the remaining overlaps.

In terms of the scaled quantities, the constraint (2.1.7) can now be written as

$$\Delta_0 = \bar{q}_1\bar{q}_2\bar{q}_3 - \bar{q}_1\bar{s}_1^2 - \bar{q}_2\bar{s}_2^2 - \bar{q}_3\bar{s}_3^2 + 2\bar{s}_1\bar{s}_2\bar{s}_3\cos\phi \geq 0 \tag{2.2.9}$$

with the equal sign representing the optimum solution. The positivity of

the principal minors of C becomes

$$\begin{aligned}
\Delta_{12} &= \bar{q}_1\bar{q}_2 - \bar{s}_3^2 \geq 0, \\
\Delta_{13} &= \bar{q}_1\bar{q}_3 - \bar{s}_2^2 \geq 0, \\
\Delta_{23} &= \bar{q}_2\bar{q}_3 - \bar{s}_1^2 \geq 0.
\end{aligned} \tag{2.2.10}$$

For the minimization of the total failure probability we take a Lagrange multiplier approach again, using the above scaled form of the constraint,

$$Q' = \sum_i \bar{q}_i + \lambda\Delta_0. \tag{2.2.11}$$

Optimization with respect to the failure probabilities leads to the equations,

$$\begin{aligned}
\frac{\partial Q'}{\partial \bar{q}_1} &= 1 + \lambda\left(\bar{q}_2\bar{q}_3 - \bar{s}_1^2\right) = 0, \\
\frac{\partial Q'}{\partial \bar{q}_2} &= 1 + \lambda\left(\bar{q}_1\bar{q}_3 - \bar{s}_2^2\right) = 0, \\
\frac{\partial Q'}{\partial \bar{q}_2} &= 1 + \lambda\left(\bar{q}_1\bar{q}_2 - \bar{s}_3^2\right) = 0.
\end{aligned} \tag{2.2.12}$$

If we solve these equations for the individual failure probabilities, we get

$$\begin{aligned}
\bar{q}_1 &= \sqrt{\frac{\left(\bar{s}_2^2 + \delta\right)\left(\bar{s}_3^2 + \delta\right)}{\left(\bar{s}_1^2 + \delta\right)}}, \\
\bar{q}_2 &= \sqrt{\frac{\left(\bar{s}_1^2 + \delta\right)\left(\bar{s}_3^2 + \delta\right)}{\left(\bar{s}_2^2 + \delta\right)}}, \\
\bar{q}_3 &= \sqrt{\frac{\left(\bar{s}_1^2 + \delta\right)\left(\bar{s}_2^2 + \delta\right)}{\left(\bar{s}_3^2 + \delta\right)}}
\end{aligned} \tag{2.2.13}$$

where we replaced $-\frac{1}{\lambda}$ with $\delta \geq 0$. These equations can also be obtained in

a straightforward manner by replacing the prior probabilities with 1 and all other parameters with their scaled versions in Eqs. (2.1.11) and (2.1.12).

The main benefit from the scaling is that Eqs. (2.2.7), (2.2.9) and (2.2.10) are now all independent of the prior probabilities. Of course, there is a price to pay: the validity range of the solutions will now explicitly depend on the prior probabilities. Nevertheless, this type of scaling will prove to be useful in extending the validity of some of the analytical solutions for special cases to a very broad range of parameters.

2.3 Quantification of the Linear Independence (LI) condition

2.3.1 General description of the LI condition

The necessary and sufficient condition for USD to be possible is that the states are linearly independent (LI) [46, 47, 48]. This condition can be quantified and will give limitations for the set of parameters s_j and ϕ.

We can construct the Gram matrix G from the state vectors such that

$$G_{ij} = \langle \psi_i | \psi_j \rangle \tag{2.3.1}$$

and $i, j = 1, 2, 3$. The geometric meaning of the Gram matrix is that its determinant is the square of the volume of the parallelepiped spanned by the three vectors in Eq. (2.0.1). If this volume is zero, the vectors lie in a plane. Thus, the condition for linear independence of the initial states $|\psi_i\rangle$ is satisfied when the determinant of the Gram matrix is larger than zero

[92],

$$\det(G) > 0. \tag{2.3.2}$$

We can write the matrix explicitly as

$$G = \begin{bmatrix} 1 & \langle\psi_1|\psi_2\rangle & \langle\psi_1|\psi_3\rangle \\ \langle\psi_2|\psi_1\rangle & 1 & \langle\psi_2|\psi_3\rangle \\ \langle\psi_3|\psi_1\rangle & \langle\psi_3|\psi_2\rangle & 1 \end{bmatrix}.$$

Then the constraint (2.3.2) becomes

$$\begin{aligned} \det(G) &= 1 - |\langle\psi_2|\psi_3\rangle|^2 - |\langle\psi_1|\psi_2\rangle|^2 - |\langle\psi_3|\psi_1\rangle|^2 \\ &\quad +2Re\left(\langle\psi_1|\psi_2\rangle\langle\psi_2|\psi_3\rangle\langle\psi_3|\psi_1\rangle\right) > 0. \end{aligned} \tag{2.3.3}$$

Substituting (2.0.1) in (2.3.3) we obtain

$$1 - s_1^2 - s_3^2 - s_2^2 + 2s_1 s_2 s_3 \cos\phi > 0 \tag{2.3.4}$$

where Eq. (2.0.2) was used. Setting Eq. (2.3.4) equal to zero we have

$$1 - s_1^2 - s_3^2 - s_2^2 + 2s_1 s_2 s_3 \cos\phi = 0. \tag{2.3.5}$$

Solving for the amplitudes s_i gives

$$\begin{aligned} s_1 &= s_3 s_2 \cos\phi \pm \sqrt{s_3^2 s_2^2 \cos^2\phi + \left(1 - s_2^2 - s_3^2\right)}, \\ s_2 &= s_3 s_1 \cos\phi \pm \sqrt{s_3^2 s_1^2 \cos^2\phi + \left(1 - s_1^2 - s_3^2\right)}, \\ s_3 &= s_1 s_2 \cos\phi \pm \sqrt{s_1^2 s_2^2 \cos^2\phi + \left(1 - s_2^2 - s_1^2\right)}. \end{aligned} \tag{2.3.6}$$

For a given fixed value of the cocycle ϕ, these equations describe a surface in the three dimensional space of s_1, s_2 and s_3. Linearly independent states will have amplitudes from 0 to the surface. Values of the amplitudes that are on the surface describe linearly dependent states. Values above the surface are impossible. In Fig. 2.1 we show solutions of (2.5.2) for different values of the cocycle ϕ.

We can understand the character of these surfaces in simple terms. Notice that when the last term in (2.3.5) is equal to 0, or equivalently $\phi = \frac{\pi}{2}$, (2.3.5) becomes the equation of the unit sphere. Having only positive values for the s_i, the boundary is described by the portion of the sphere in the first octant (Fig. 2.1a). If we vary the value of ϕ starting from $\frac{\pi}{2}$, the surface is distorted nonuniformly, in such a way that the distortion is largest along the main diagonal starting at the origin and running toward the corner $(1, 1, 1)$ while there is no distortion in the three planes bounding the positive octant. The latter can be seen by substituting $s_1 = 0$ (or, equivalently, $s_2 = 0$ or $s_3 = 0$) in Eq. 2.5.2 in which case it describes a quarter circle in the bounding plane orthogonal to s_1 (or s_2 or s_3). If the value of ϕ starting from $\frac{\pi}{2}$ is decreased the sphere stretches out more and more until it reaches the corner $(1, 1, 1)$ for $\phi = 0$ (Fig. 2.1b). On the other hand, increasing the value

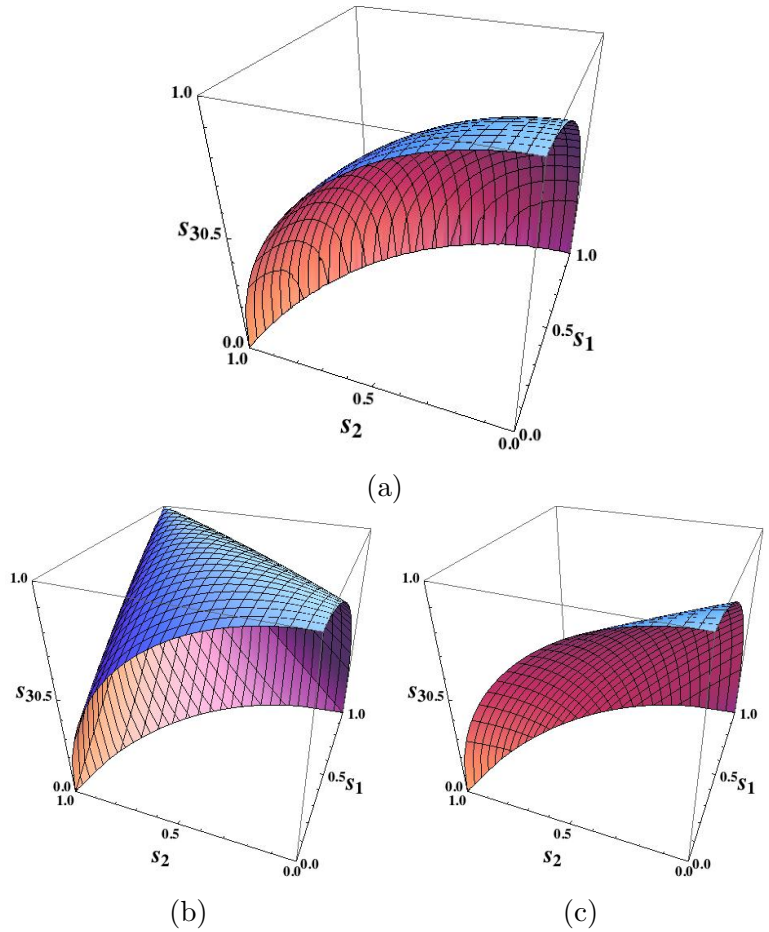

Figure 2.1: General surface (2.5.2) when the cocycle a) $\phi = \frac{\pi}{2}$ b) $\phi = 0$ and c) $\phi = \pi$.

of ϕ, again starting from $\frac{\pi}{2}$, the spherical surface is compressed until the enclosed volume is at its minimum for $\phi = \pi$ (Fig. 2.1c). Thus, increasing or decreasing the value of ϕ starting from $\phi = \pi/2$ will stretch or compress the sphere along the main diagonal in such a way that its intersections with the coordinate planes remain undistorted.

2.3.2 Illustration of the Linear Independence condition for special cases

The behavior of the linear independence condition will be illustrated for two special cases.

Three equal amplitudes

First, let us consider the case were the mutual overlaps are all equal. We are interested in the maximum allowed value of the overlap amplitude as we change its value along the diagonal pointing from the origin toward the corner $(1,1,1)$ in Figs. 2.1a - 2.1c, as a function of the cocycle ϕ. Substituting $s_1 = s_2 = s_3 = s$ into Eq. (2.3.5), we obtain

$$2s^3 \cos\phi - 3s^2 + 1 = 0, \tag{2.3.7}$$

with the solutions

$$s_{max} = \begin{cases} \frac{1}{2\cos\frac{\pi-\phi}{3}} & \text{if } 0 \leq \phi < 2\pi \ , \\ -\frac{1}{\cos\phi/3} & \text{if } 2\pi \leq \phi < 4\pi \ , \\ \frac{1}{2\cos\frac{\pi+\phi}{3}} & \text{if } 4\pi \leq \phi < 6\pi \ . \end{cases} \tag{2.3.8}$$

This expression is a special case of the more general case of n symmetric states as recently obtained by [56]. It should also be noted that the three lines in Eq. (2.3.8) correspond to just one 2π-periodic solution, only the analytical expressions are different in the various 2π intervals because the cubic equation (2.3.7) has a 6π periodicity.

Thus, for the case when all amplitudes are equal, permissible values of s lie on the diagonal line connecting the origin to the corner $(1, 1, 1)$ and are bounded by the origin on one end and the intersection of the diagonal with the bounding surface on the other, i.e. $0 \leq s < s_{max}$.

Let us explore some specific values of ϕ. Starting with $\phi = 0$ we have $0 \leq s < 1$, i.e. the entire diagonal is permitted, except the endpoint at $s = 1$. Increasing the value of the cocycle ϕ to $\frac{\pi}{2}$, decreases the permissible range of s to $0 \leq s < 1/\sqrt{3}$. The upper bound in this case is simply the intersection of the diagonal with the unit sphere (see Fig. 2.1a). The smallest upper bound is reached for $\phi = \pi$, where the range for permissible values is $0 \leq s < 1/2$. The full range of s as a function of ϕ from $0 \leq \phi \leq 2\pi$ is displayed in Fig. 2.2.

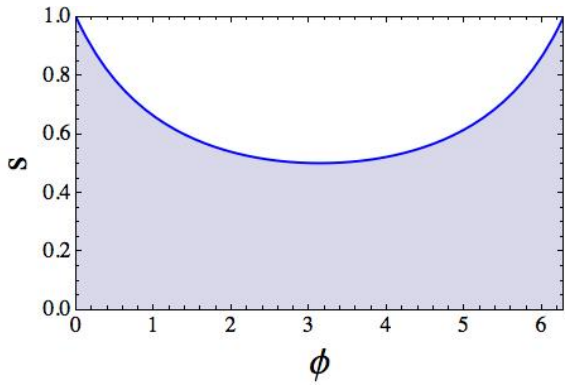

Figure 2.2: For the states to be linearly independent, permissible values for s vs. ϕ are represented by the shaded area for the case when all overlaps are equal. The upper boundary of the permissible region is given by the first line in Eq. (2.3.8) for the $0 \leq \phi \leq 2\pi$ interval.

Two equal amplitudes

Without loss of generality, we assume $s_1 = s_2 \equiv s$ and $s_3 \neq s$ in (2.0.1). Substituting these into Eq. (2.3.5), the states will be linearly dependent if

$$2s^2 s_3 \cos\phi - 2s^2 - s_3^2 + 1 = 0. \tag{2.3.9}$$

This defines the boundary surface for $s_3(s, \phi)$,

$$s_3^{(\pm)} = s^2 \cos\phi \pm \sqrt{s^4 \cos^2\phi + (1 - 2s^2)} \tag{2.3.10}$$

within which permissible values of the amplitudes s and s_3 and the cocycle ϕ lie for linearly independent states. The boundary surface is displayed in Fig. 2.3.

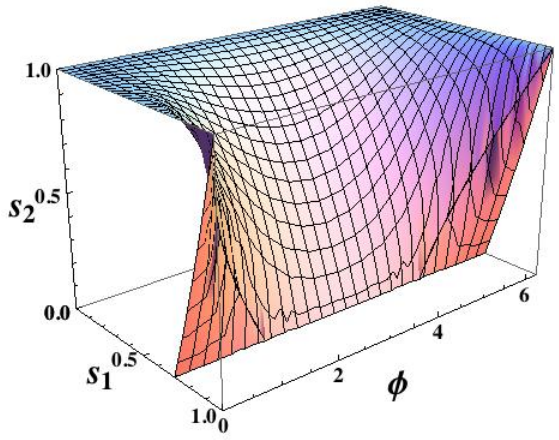

Figure 2.3: Boundary surface for permissible values of s_3 as a function of s and the cocycle ϕ.

One can take a different look at the same information; a parametric plot in this case is more revealing. The case of two equal overlap amplitudes

corresponds to the diagonal plane $s_1 = s_2 = s$ in Fig. 2.1. The permissible states now lie in this plane and their upper boundary is given by the line intersection of the plane with the boundary surface. This boundary line is displayed for representative values of ϕ in Fig. 2.4.

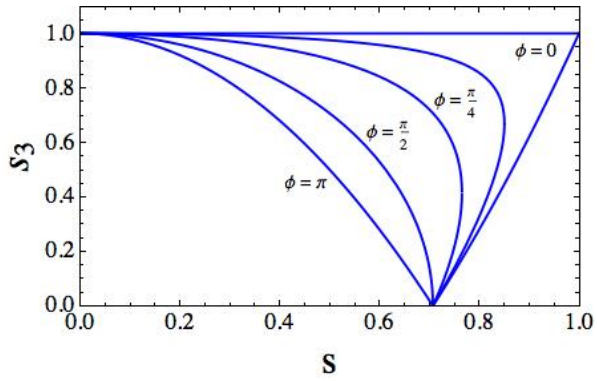

Figure 2.4: Boundary lines for permissible values of s_3 as a function of s for representative values of ϕ.

It is again apparent from both Fig. 2.3 and Fig. 2.4 that the surface is compressed as the value of the cocycle ϕ is increased from 0 to π.

In addition, the character of the boundary changes at $s = 1/\sqrt{2}$ and $\phi = \pi/2$, from single-valued to bivalued. We see from Eq. (2.3.10) that the boundary line has two branches, $s_3^{(+)}$ which is always positive and $s_3^{(-)}$ which is negative if $s < 1/\sqrt{2}$ and positive if $s > 1/\sqrt{2}$. Permissible values for s_3 are such that $s_3^{(+)} > s_3 \geq max\{0, s_3^{(-)}\}$. Furthermore, the value of s is bounded by s_{max} for a given ϕ. For s_3 to be real the discriminant $d = s^4 \cos^2\phi + \left(1 - 2s^2\right)$ has to be larger than or equal to zero. At $d = 0$ the two branches merge continuously and this defines s_{max}, the maximum permissible value of s for a fixed $0 < \phi < \pi/2$ in Eq. (2.3.9), while $s_{max} =$

$1/\sqrt{2}$ in the interval $\pi/2 < \phi < \pi$, independently of ϕ,

$$s_{max} = \begin{cases} \frac{1}{\sqrt{1+\sin\phi}} & \text{if } 0 \leq \phi < \pi/2 \ , \\ \frac{1}{\sqrt{2}} & \text{if } \pi/2 \leq \phi < \pi \ . \end{cases} \tag{2.3.11}$$

Inserting s_{max} from Eq. (2.3.11) into Eq. (2.3.10), yields

$$s_3 = \begin{cases} \frac{\cos\phi}{1+\sin\phi} & \text{if } 0 \leq \phi < \pi/2 \ , \\ 0 & \text{if } \pi/2 \leq \phi < \pi \ . \end{cases} \tag{2.3.12}$$

for the corresponding values of s_3 at the right asymptotic point s_{max}.

2.3.3 Linear Independence condition in scaled quantities

It is particularly revealing to represent the LI condition in scaled quantities from Eq. (2.2.1). After dividing Eq. (2.3.4) by $s_1 s_2 s_3$ we get

$$r_1 r_2 r_3 - r_1 - r_2 - r_3 + 2\cos\phi > 0. \tag{2.3.13}$$

Equality in the above equation, for a given fixed value of the Berry phase ϕ, defines a smooth (hyperbolic) surface in the positive octant of the three dimensional space of r_1, r_2 and r_3. Linearly independent states correspond to points above the surface, thus they form a convex set. Points that are on the surface describe linearly dependent states. Points below the surface are impossible. The set of LI states is displayed in Fiq. 2.5 for $\phi = 0$. As we increase ϕ from 0 to π the boundary surface moves away from the origin along the main diagonal and gets more rounded around the apex. The apex is the

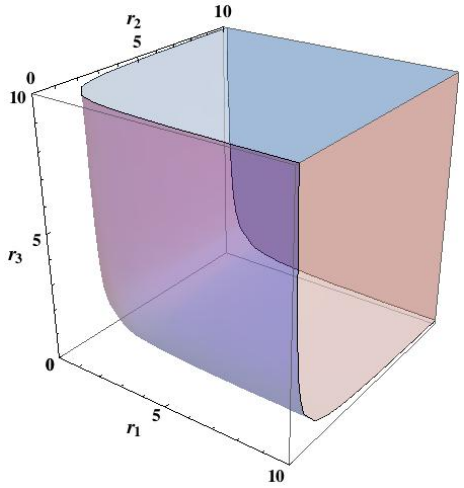

Figure 2.5: The convex set of linearly independent states.

point closest to the origin and its coordinates are $r_1 = r_2 = r_3 = 2\cos(\frac{\pi-\phi}{3})$.

The boundary surface as well as the convex set of permissible LI states will play a key role in developing a complete geometric view of the problem.

2.4 Geometric interpretation of the optimum solution

The aforementioned Scaling A will be used to present a geometric picture of the optimum solution of the USD of three non-orthogonal states.

Recall that the LI condition in terms of the r_i parameters from Eq. (2.2.1) is

$$r_1 r_2 r_3 - r_1 - r_2 - r_3 + 2\cos\phi > 0. \tag{2.3.13}$$

The constraint for the optimum solution of the USD in the same scaling is

$$\tilde{q}_1\tilde{q}_2\tilde{q}_3 - \tilde{q}_1 - \tilde{q}_2 - \tilde{q}_3 + 2\cos\phi \geq 0. \tag{2.2.3}$$

The similarity of these two equations is striking; the two relations can be displayed in the same plot if we exchange the labels of the axes $\{r_1, r_2, r_3\}$ in Fig. 2.5 with $\{\tilde{q}_1, \tilde{q}_2, \tilde{q}_3\}$. While the permissible values for the LI condition lie strictly above the surface, points on and above the surface represent possible failure probabilities.

Let us also recall the total failure probability in terms of the r_i parameters

$$Q = \sum_{i=1}^{3} \eta_i \frac{\tilde{q}_i}{r_i}. \tag{2.2.4}$$

The original failure probabilities $q_i \leq 1$. This translates to $\tilde{q}_i \leq r_i$ for the scaled quantities using (2.2.2). Therefore possible solutions to Eq. (2.2.3) lie within a volume bounded by the surface given by the equal sign in Eq. (2.2.3) and by the intersection of the $\{\tilde{q}_i = r_i | i = 1, 2, 3\}$ planes with that surface. This bounded volume is called the *feasible set*. The solution is optimum if the equal sign in Eq. (2.2.3) holds. Hence, optimal values for the failure probabilities lie on the boundary surface (Eq. (2.2.3)) itself. This is called the *optimal feasible set*. It is easy to check that the boundary lines of the optimal feasible set are hyperbolas. For some representative values of $\{r_i\}$ and ϕ, the situation is illustrated in Fig. 2.6.

In order to find the actual solution on the closed surface area of the optimal feasible set in Fig. 2.6, let us notice that for a fixed Q and given prior probabilities and overlaps, Eq. (2.2.4) is a plane in the 3D configuration

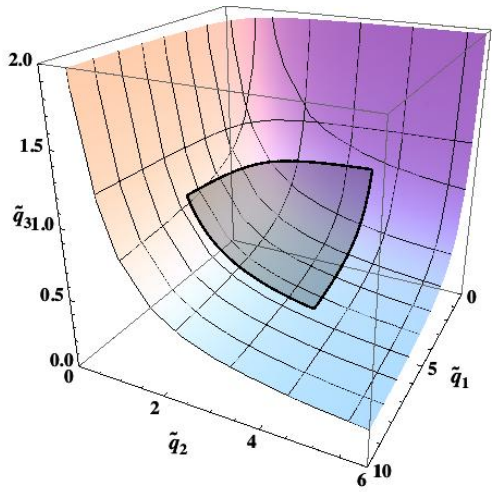

Figure 2.6: Optimal feasible set (shaded area), the range of possible solutions for $\{\tilde{q}_i\}$ for $r_1 = 6.25$, $r_2 = 4$, $r_3 = 1$ and $2\cos\phi = \sqrt{3}/2$. The boundary lines are hyperbolas in the $\{\tilde{q}_i, \tilde{q}_j | i \neq j\}$ planes. The feasible set is a bounded volume above the surface.

space of Figs. 2.5 and 2.6, spanned by $\{\tilde{q}_i\}$. Its intersections with the axes are given by $\tilde{q}_i = Qr_i/\eta_i$, so it is a tilted triangle in the positive octant, shown in Fig. 2.7.

Solutions to the state discrimination problem are the points that are simultaneously in the optimal feasible set of Fig. 2.6 and the plane of Fig. 2.7. If Q is chosen too small, as is intentionally the case in Fig. 2.7, the plane will be entirely under the area occupied by the feasible set and there is no solution to the problem. As we increase the value of Q, there will be a smallest value, Q_{opt} for which the two surfaces develop a common point and the coordinates of this point represent the optimum individual failure probabilities, $\{q_{i,opt} = \tilde{q}_{i,opt}/r_i\}$. Hence, this point *is* the optimal solution to the unambiguous discrimination problem. If we increase Q beyond its

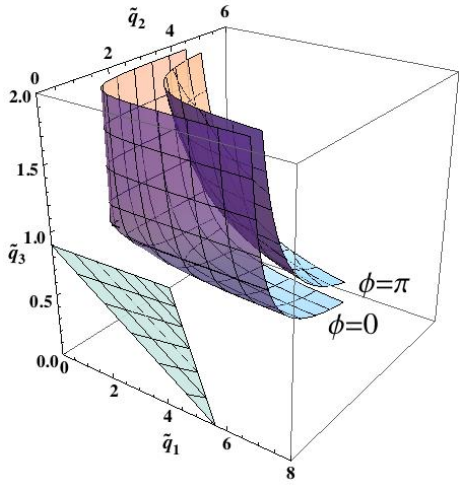

Figure 2.7: Plane corresponding to the average failure probability, Eq. (2.2.4), in the positive octant of the $\{\tilde{q}_i\}$ space, for $Q = 0.3$ and $\eta_i = 1/3$. Other parameters, $r_1 = 6.25$, $r_2 = 4$ and $r_3 = 1$, are the same as in Fig. 2.6.

optimal value then several solutions are possible corresponding to a given $Q > Q_{opt}$ but they are clearly not optimal.

On the other hand the optimal value of Q increases for increasing ϕ starting at $\phi = 0$ and reaches its maximum for $\phi = \pi$. However the general features of the solution stay the same. The surface of the optimal feasible set becomes more rounded around the apex for increasing ϕ.

We have now a complete and intuitive geometric view of the optimum solution which can be classified into three categories depending on the position of the common point. The common point can be inside the surface area, on the boundary line or at one of the vertices where two boundary lines meet. This can be interpreted in terms of solutions as follows

- *Interior point.* All three of the failure probabilities are such that $\tilde{q}_i < r_i$ which means that $q_i < 1$. In this case all three of the states can be

unambiguously discriminated with finite probability of success.

- *Boundary point.* Since the boundary lines are hyperbola with $\tilde{q}_i = r_i$ where $i = 1, 2, 3$ one of the $q_i = 1$ and the state $|\psi_i\rangle$ cannot be discriminated unambiguously, while the other two states can be discriminated with finite probability of success.

- *Vertex.* This is the point where two hyperbolas corresponding to $\tilde{q}_i = r_i$ and $\tilde{q}_j = r_j$ meet where i and $j \neq i$ are from the set $\{1, 2, 3\}$. Then $q_i = q_j = 1$ and the states $|\psi_i\rangle$ and $|\psi_j\rangle$ cannot be discriminated unambiguously, while the remaining third state can be discriminated with finite probability of success. Note that this is the worst case scenario, at least one out of three linearly independent states can always be discriminated unambiguously.

2.5 Analytical Solutions for some special cases

In this section we present analytical solutions for some special cases. We will use Eqs. (2.1.7), (2.1.9) and (2.1.12) if we use the original parameters, Eqs. (2.2.3) and (2.2.5) if Scaling A is used and Eqs. (2.2.9), (2.2.10) and (2.2.13) if Scaling B is used.

We demonstrate the power of Scaling B by giving the complete solution for arbitrary amplitudes and priors for $\phi = 0$. Since, as demonstrated in the geometric solution qualitatively, increasing ϕ will increase Q_{opt} without altering other features the $\phi = 0$ case will serve as a representative of the universal features of the optimal solution. We call this the *real state case*

even so $\phi = 0$ also encompasses cases where the complex overlaps satisfy $\phi_{12} + \phi_{23} + \phi_{31} = 0$ without all of them being equal to zero. We will relate the analytical solutions to the categories of solutions in the geometric interpretation. The validity range of the solutions is also illustrated.

Continuing with the simple case where all three overlap amplitudes and prior probabilities are equal we derive the complete solution for arbitrary ϕ. We will parallel the former case with a congruent treatment with scaled quantities using Scaling B. While both solutions have the same structure the range of validity is greatly extended in the latter. Furthermore we present the case of two equal amplitudes and arbitrary ϕ.

Equal probability or weighted equal probability measurements (EPM or WEPM) are always possible. While they are in general suboptimal solutions these measurements can become optimal if the prior probabilities are adjusted. We explore the necessary conditions for those cases.

All these cases attack the problem of unambiguous discrimination of three, pure, non-orthogonal states from different sides: first, by setting the cocycle $\phi = 0$ and keeping the overlaps and prior probabilities arbitrary, second, by fixing the relationship between the overlaps but keeping ϕ arbitrary and third, by having arbitrary overlaps and ϕ, and adjusting the a priori probabilities. Only, in the most general case, with all overlap amplitudes different, all prior probabilities different and $\phi \neq 0$, the problem eludes the analytical treatment.

2.5.1 Real states and phase transition

We now present the full solution for the case of vanishing Berry phase $\phi = 0$ using Scaling B from Sec. 2.2. Although this covers states with complex overlaps satisfying that the sum of their phases vanish, $\phi_{12}+\phi_{23}+\phi_{31} = 0$, for simplicity, we refer to these states as real. In terms of the scaled quantities, the constraint can be written as

$$\Delta_0 = \bar{q}_1\bar{q}_2\bar{q}_3 - \bar{q}_1\bar{s}_1^2 - \bar{q}_2\bar{s}_2^2 - \bar{q}_3\bar{s}_3^2 + 2\bar{s}_1\bar{s}_2\bar{s}_3 = 0. \tag{2.5.1}$$

The individual failure probabilities from Eq. (2.2.13) are

$$\begin{aligned}
\bar{q}_1 &= \sqrt{\frac{\left(\bar{s}_2^2+\delta\right)\left(\bar{s}_3^2+\delta\right)}{\left(\bar{s}_1^2+\delta\right)}}, \\
\bar{q}_2 &= \sqrt{\frac{\left(\bar{s}_1^2+\delta\right)\left(\bar{s}_3^2+\delta\right)}{\left(\bar{s}_2^2+\delta\right)}}, \\
\bar{q}_3 &= \sqrt{\frac{\left(\bar{s}_1^2+\delta\right)\left(\bar{s}_2^2+\delta\right)}{\left(\bar{s}_3^2+\delta\right)}}
\end{aligned} \tag{2.5.2}$$

Substituting Eqs. (2.2.13) into Eq. (2.5.1) will result in a sixth-order equation with two of the solutions being $\delta = 0$. After separating these solutions, a fourth-order equation results for the $\delta \neq 0$ solutions, which is a great simplification compared to the non-separable sixth-order equation of the general

$\phi \neq 0$ case,

$$\begin{aligned} \delta^4 &- 2(\bar{s}_1^2\bar{s}_2^2 + \bar{s}_2^2\bar{s}_3^2 + \bar{s}_3^2\bar{s}_1^2)\delta^2 - 8\bar{s}_1^2\bar{s}_2^2\bar{s}_3^2\delta \\ &+ \bar{s}_1^4\bar{s}_2^4 + \bar{s}_2^4\bar{s}_3^4 + \bar{s}_3^4\bar{s}_1^4 \\ &- 2\bar{s}_1^2\bar{s}_2^2\bar{s}_3^2(\bar{s}_1^2 + \bar{s}_2^2 + \bar{s}_3^2) = 0, \end{aligned} \tag{2.5.3}$$

This equation has four solutions. Together with the zero solution we have five that may be physically acceptable for some values of the parameters. They are

$$\begin{aligned} \delta_1 &= 0, \\ \delta_2 &= \bar{s}_1\bar{s}_2 - \bar{s}_2\bar{s}_3 - \bar{s}_3\bar{s}_1 \quad \text{if } \delta_2 \geq 0, \\ \delta_3 &= \bar{s}_2\bar{s}_3 - \bar{s}_3\bar{s}_1 - \bar{s}_1\bar{s}_2 \quad \text{if } \delta_3 \geq 0, \\ \delta_4 &= \bar{s}_3\bar{s}_1 - \bar{s}_1\bar{s}_2 - \bar{s}_2\bar{s}_3 \quad \text{if } \delta_4 \geq 0, \\ \delta_5 &= \bar{s}_1\bar{s}_2 + \bar{s}_2\bar{s}_3 + \bar{s}_3\bar{s}_1. \end{aligned} \tag{2.5.4}$$

Eq. (2.5.3) contains the last term from Eq. (2.5.1), $2\bar{s}_1\bar{s}_2\bar{s}_3$ squared. Therefore, Eq. (2.5.3) is equally valid for $\phi = \pi$, which would appear with a minus sign in for the last term in Eq. (2.5.3). It turns out that solution δ_5 is indeed the solution to the $\phi = \pi$ case and satisfies the constraint in Eq. (2.5.3). On the other hand, out of the three solutions, δ_2, δ_3, and δ_4, only at most one can be positive for a given parameter set. However, it is possible that all three are negative simultaneously in which case δ_1 is the only physically acceptable solutions.

Substituting $\delta = \delta_1 = 0$ into Eq. (2.2.13) yields

$$\begin{aligned} \bar{q}_1^{(1)} &= \frac{\bar{s}_2\bar{s}_3}{\bar{s}_1}, \\ \bar{q}_2^{(1)} &= \frac{\bar{s}_3\bar{s}_1}{\bar{s}_2}, \\ \bar{q}_3^{(1)} &= \frac{\bar{s}_1\bar{s}_2}{\bar{s}_3}. \end{aligned} \tag{2.5.5}$$

The sub-determinants of C give no further limits in this case, they are all equal zero.

In Table 2.1 we present all five sets of the failure probabilities corresponding to the five solutions for δ in Eq. (2.5.4).

δ_i	$\bar{q}_1^{(i)}$	$\bar{q}_2^{(i)}$	$\bar{q}_3^{(i)}$
δ_1	$\frac{\bar{s}_2\bar{s}_3}{\bar{s}_1}$	$\frac{\bar{s}_3\bar{s}_1}{\bar{s}_2}$	$\frac{\bar{s}_1\bar{s}_2}{\bar{s}_3}$
δ_2	$\bar{s}_2 - \bar{s}_3$	$\bar{s}_1 - \bar{s}_3$	$\bar{s}_1 + \bar{s}_2$
δ_3	$\bar{s}_2 + \bar{s}_3$	$\bar{s}_3 - \bar{s}_1$	$\bar{s}_2 - \bar{s}_1$
δ_4	$\bar{s}_3 - \bar{s}_2$	$\bar{s}_1 + \bar{s}_3$	$\bar{s}_1 - \bar{s}_2$
δ_5	$\bar{s}_2 + \bar{s}_3$	$\bar{s}_1 + \bar{s}_3$	$\bar{s}_1 + \bar{s}_2$

Table 2.1: The five possible sets of failure probabilities for unambiguous discrimination of three linearly independent real states.

The δ_1 row is, of course, the set given in the Eq. (2.5.5) above. For the solution δ_2 the positivity of the sub-determinants of C gives

$$\bar{s}_1\bar{s}_2 - \bar{s}_3(\bar{s}_1 + \bar{s}_2) \geq 0. \tag{2.5.6}$$

This coincides with the threshold condition for the existence of the δ_2 type solution. The positivity of the sub-determinants yield similar equations for the δ_3 and δ_4 solutions. The δ_5 solution, although unconditionally positive,

will lead to a maximum of Q, therefore it can be left out from further consideration.

For a given set of parameters only one of the remaining solutions can be optimal and we are interested in finding out which. The $\delta_0 = 0$ solution exists unconditionally, for any value of the parameters. Thus, either it exists alone for a given set of parameters or it coexists with one of the other three solutions.

With no loss of generality we assume $\bar{s}_1 \geq \bar{s}_2 \geq \bar{s}_3$ in the discussion that follows, since this can always be arranged by simply renumbering the states. Therefore, it is sufficient to consider the two sets of solutions for δ_1 and δ_2. Because of this ordering, we are interested in the effect of changing $\bar{s}_3$ while keeping $\bar{s}_1$ and $\bar{s}_2$ fixed. We consider two regimes depending on whether $\bar{s}_3$ is smaller or larger than the threshold value for the existence of the δ_2 solution

$$\bar{s}_3^{th} = \frac{\bar{s}_1 \bar{s}_2}{\bar{s}_1 + \bar{s}_2} \tag{2.5.7}$$

If we have $\bar{s}_3 > \bar{s}_3^{th}$ then δ_1 is the only solution. Starting with a situation where all $\bar{q}_i^{(1)} \leq \eta_i$ we vary $\bar{s}_3$. First, we increase $\bar{s}_3$ and $\bar{q}_3^{(1)}$ decreases. Since $\bar{q}_1^{(1)}$ and $\bar{q}_2^{(1)}$ depend linearly on $\bar{s}_3$ they increase. It might happen that either $\bar{q}_1$ eventually becomes equal to η_1 or $\bar{q}_2$ eventually becomes equal to η_2. At this point either $q_1 = 1$ or $q_2 = 1$ and we are on the border of the boundary area in Fig. 2.7. The state $|\psi_1\rangle$ or $|\psi_2\rangle$ can no longer be unambiguously discriminated which means that the POVM element Π_0, corresponding to failure, must contain the full $|\psi_1\rangle\langle\psi_1|$ or $|\psi_2\rangle\langle\psi_2|$ projector, respectively. Note however that at most one of the $\bar{q}_i$'s can become equal to the the

corresponding η_i. To see this let us use the original, unscaled parameters s_i and corresponding $q_i^{(1)}$. The conditions for $q_i^{(1)} = 1$ are

$$\begin{aligned} q_1^{(1)} &= 1 \quad \text{if} \quad s_1 = s_2 s_3 \\ q_2^{(1)} &= 1 \quad \text{if} \quad s_2 = s_1 s_3 \\ q_3^{(1)} &= 1 \quad \text{if} \quad s_3 = s_1 s_2 \end{aligned} \tag{2.5.8}$$

Clearly, either $q_1^{(1)}$ or $q_2^{(1)}$ can be equal to 1 for fixed s_1 and s_2 unless $s_1 = s_2$ and $s_3 = 1$ which means that $|\psi_1\rangle$ and $|\psi_2\rangle$ are linearly dependent, contradicting our assumption of linear independence. Therefore, at most one of the $\bar{q}_i$'s can become equal to the corresponding η_i and no vertex solution exists in this case.

Starting again from a situation where $\bar{q}_i^{(1)} \leq \eta_i$ we decrease $\bar{s}_3$. Now one of two things can happen. If $\eta_3 < \bar{s}_1 + \bar{s}_2$ the only valid solution is the δ_1 solution since $\bar{q}_3^{(2)} > \eta_3$ or, equivalently, $q_3 > 1$ are not possible. Decreasing $\bar{s}_3$ further $\bar{q}_3^{(1)}$ would eventually become equal to η_3 and $|\psi_3\rangle$ can no longer be unambiguously discriminated.

On the other hand, if $\eta_3 > \bar{s}_1 + \bar{s}_2$ decreasing $\bar{s}_3$ further $\bar{q}_3^{(1)}$ would eventually become equal to $\bar{s}_1 + \bar{s}_2$. This happens when $\bar{s}_3 = \bar{s}_3^{th}$ and we have $\delta_1 = \delta_2 = 0$. This is a branch point and decreasing $\bar{s}_3$ further both the $\bar{q}_i^{(1)}$ and $\bar{q}_i^{(2)}$ type solutions will exist. Here, $\bar{q}_3^{(1)}$ would eventually become equal to η_3 and $|\psi_3\rangle$ can no longer be unambiguously discriminated.

On the contrary, $\bar{q}_3^{(2)}$ is independent of $\bar{s}_3$ and remains at its fixed value $\bar{q}_3^{(2)} = \bar{s}_1 + \bar{s}_2$. However, $\bar{q}_1^{(2)}$ and $\bar{q}_2^{(2)}$ actually increase. Therefore, it is possible in this region that we first reach, say, $\bar{q}_1^{(2)} = \eta_1$ (if $\bar{s}_2 > \eta_1$ which

is possible if $\eta_3 > \eta_1$) and then $\bar{q}_2^{(2)} = \eta_2$ (if $\bar{s}_1 > \eta_2$ which is possible if $\eta_3 > \eta_2$) by lowering $\bar{s}_3$ further. So, starting from a point inside the feasible region, we first have a phase transition, then the point moves to the border of the feasible region and, finally, to the vertex $\bar{q}_1^{(2)} = \eta_1$ and $\bar{q}_2^{(2)} = \eta_2$ along the border. The condition for such behavior to exist is, clearly, $\bar{s}_2^{(2)} \geq \eta_1$ and $\bar{s}_1^{(2)} \geq \eta_2$. Adding these two conditions gives $\bar{s}_1^{(2)} + \bar{s}_2^{(2)} \geq \eta_1 + \eta_2 = 1 - \eta_3$. Taking into account that $\eta_3 > \bar{s}_1 + \bar{s}_2$ for this type of solution to exist, we obtain $\eta_3 > 1/2$ as the overall existence condition for a vertex solution.

The solutions are summarized in Tables 2.2 and 2.3.

$Q_{opt}^{(1)} =$	**if**
$\frac{\bar{s}_2\bar{s}_3}{\bar{s}_1} + \frac{\bar{s}_3\bar{s}_1}{\bar{s}_2} + \frac{\bar{s}_1\bar{s}_2}{\bar{s}_3}$	$\frac{\bar{s}_2\bar{s}_3}{\bar{s}_1} < \eta_1 \quad \frac{\bar{s}_3\bar{s}_1}{\bar{s}_2} < \eta_2 \quad \frac{\bar{s}_1\bar{s}_2}{\bar{s}_3} < \eta_3$
$\eta_1 + \frac{\bar{s}_3\bar{s}_1}{\bar{s}_2} + \frac{\bar{s}_1\bar{s}_2}{\bar{s}_3}$	$\frac{\bar{s}_2\bar{s}_3}{\bar{s}_1} \geq \eta_1 \quad \frac{\bar{s}_3\bar{s}_1}{\bar{s}_2} < \eta_2 \quad \frac{\bar{s}_1\bar{s}_2}{\bar{s}_3} < \eta_3$
$\frac{\bar{s}_2\bar{s}_3}{\bar{s}_1} + \eta_2 + \frac{\bar{s}_1\bar{s}_2}{\bar{s}_3}$	$\frac{\bar{s}_2\bar{s}_3}{\bar{s}_1} < \eta_1 \quad \frac{\bar{s}_3\bar{s}_1}{\bar{s}_2} \geq \eta_2 \quad \frac{\bar{s}_1\bar{s}_2}{\bar{s}_3} < \eta_3$
$\frac{\bar{s}_2\bar{s}_3}{\bar{s}_1} + \frac{\bar{s}_3\bar{s}_1}{\bar{s}_2} + \eta_3$	$\frac{\bar{s}_2\bar{s}_3}{\bar{s}_1} < \eta_1 \quad \frac{\bar{s}_3\bar{s}_1}{\bar{s}_2} < \eta_2 \quad \frac{\bar{s}_1\bar{s}_2}{\bar{s}_3} \geq \eta_3$
	i) $\bar{s}_3 = \frac{\bar{s}_1\bar{s}_2}{\eta_3} > \bar{s}_3^{th}$ if $\bar{s}_1 + \bar{s}_2 > \eta_3$
	ii) $\bar{s}_3 = \frac{\bar{s}_1\bar{s}_2}{\eta_3} < \bar{s}_3^{th}$ if $\bar{s}_1 + \bar{s}_2 < \eta_3$

Table 2.2: The optimum failure probabilities $Q_{opt}^{(1)}$for the δ_1 solution for the whole range of $\bar{s}_3$.

In Fig. 2.8 we illustrate the behavior for $\bar{s}_1 + \bar{s}_2 < \eta_3$. The optimum failure probabilities $Q^{(1)}$ and $Q^{(2)}$ are plotted vs. the unscaled s_3 for $\eta_1 = 0.45$, $\eta_2 = 0.25$, $\eta_3 = 0.3$, $s_1 = 0.5$ and $s_2 = 0.3$. The two curves are just touching for $s_3 = s_{th} = 0.182$. Of course, $Q^{(2)}$ does not exist for $s_3 > 0.182$,

$Q_{opt}^{(2)} =$	**if**	
$2(\bar{s}_1 + \bar{s}_2 - \bar{s}_3)$	$\bar{s}_2 - \bar{s}_3 < \eta_1$	$\bar{s}_1 - \bar{s}_3 < \eta_2$
$\eta_1 + 2\bar{s}_1 + \bar{s}_2 - \bar{s}_3$	$\bar{s}_2 - \bar{s}_3 \geq \eta_1$	$\bar{s}_1 - \bar{s}_3 < \eta_2$
$\bar{s}_1 + 2\bar{s}_2 - \bar{s}_3 + \eta_2$	$\bar{s}_2 - \bar{s}_3 < \eta_1$	$\bar{s}_1 - \bar{s}_3 \geq \eta_2$
$\eta_1 + \eta_2 + \bar{s}_1 + \bar{s}_2$	$\bar{s}_2 - \bar{s}_3 \geq \eta_1$	$\bar{s}_1 - \bar{s}_3 \geq \eta_2$

Table 2.3: The optimum failure probabilities $Q_{opt}^{(2)}$ for the δ_2 solution where $\bar{s}_3 \leq \bar{s}_3^{th}$ and $\eta_3 > \bar{s}_1 + \bar{s}_2$.

it is merely extended to this region to show that at the branch point the two curves also have the same slope. Clearly, for $s_3 < 0.182$ $Q^{(2)}$ is optimal for discriminating all three states. While for $s_3 < 0.15$ $q_3^{(1)} = 1$ only two states are discriminated using the δ_1 solution, the δ_2 solution continues to discriminate between all three states. This region is shown enlarged as an inset in Fig. 2.8 where the vertical lines are at $s_3 = 0.182$ and $s_3 = 0.15$. For $s_3 > 0.182$ the only existing solution is δ_1 and is also the optimal one. For $s_3 > 0.6$ we have $q_2 = 1$ and, again, only two states are discriminated.

The above results have an interesting and potentially important implication. What we have just found is an example of spontaneous symmetry breaking and a second-order phase transition at $s_3 = s_{th}$. The original problem has permutational symmetry: it is invariant under the simultaneous permutation of the indexes numbering the parameters and the states. The δ_1 set of solutions, $q_i^{(1)}$ and $Q^{(1)}$, possesses this feature. However, failure probabilities in the δ_2 set are not invariant under permutation of the indexes. Symmetry is preserved only in the sense that the δ_2, δ_3 and δ_4 sets

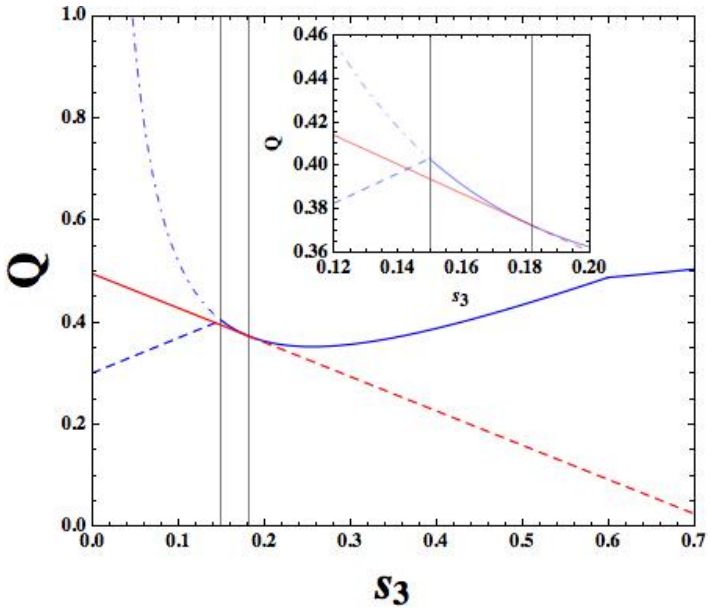

Figure 2.8: $Q^{(1)}$ and $Q^{(2)}$ vs. s_3 plotted together, for $\eta_1 = 0.45$, $\eta_2 = 0.25$, $\eta_3 = 0.3$, $s_1 = 0.5$ and $s_2 = 0.3$. The two curves are just touching for $s_3 = 0.182$. Of course, $Q^{(2)}$ does not exist for $s_3 > 0.182$, it is merely extended to this region to show that at the branch point the two curves also have the same slope.

transform into one another under permutation but the symmetry is broken within a fixed set. Since the system chooses only one of these sets at the branch point, it exhibits spontaneous symmetry breaking. It is well known that true quantum phase transitions are impossible at zero temperature due to the linearity of quantum mechanics. In our case, the origin of the symmetry breaking phase transition can be traced back to the nonlinearity of the constraint, (2.1.7), expressing the positivity condition of the POVM element corresponding to inconclusive outcome.

Lastly, the range of validity of solutions from Eq. (2.5.4) is displayed within the set of linearly independent states in Figs. 2.9 for $\eta_1 = \eta_2 = \eta_3 =$

1/3 and for $\eta_1 = \eta_2 = 1/5$ and $\eta_3 = 3/5$.

For equal a priori probabilities η_i the validity range for δ_2, δ_3 and δ_4 are the same oriented along each of the axes $r1$, $r2$ and $r3$, respectively. If the a priori probabilities are skewed in favor of one of them i.e. $\eta_3 > 1/2$, as is the case in Fig. 2.9 b, one of the solutions, here δ_2 is valid for a much larger range. In both cases the δ_1 solution is valid for the whole range of linearly independent states.

In conclusion, the unambiguous discrimination of three real states with $\phi = 0$ has two kinds of optimal solutions, the completely symmetric δ_1 type solution and one where the symmetry is broken, δ_2, δ_3 and δ_4 type solutions. While the δ_1 solution is always valid it is not always optimal. In the parameter range where δ_i with $i = 2, 3, 4$ is valid δ_i is optimal as long as $q_3^{(1)} < 1$. In our example if $\bar{s}_3 \leq \bar{s}_3^{th}$ and $\eta_3 > \bar{s}_1 + \bar{s}_2$ the δ_2 solution is optimal until $q_3^{(1)} = 1$, which happens at $s_3 = 0.15$. The range of validity of δ_i with $i = 2, 3, 4$ depends on the a priori probabilities and is skewed in favor of the largest probability.

In case of the δ_1 solution at least two states will always be discriminated. The point where the Q plane touches the optimal feasible set is either an interior point or a boundary point. No vertex solution exist. On the other hand a vertex solution is possible in case of δ_i solution with $i = 2, 3, 4$.

Finally, δ_5 is the solution for the $\phi = \pi$ case. It is the only solution for the whole parameter range and completely symmetric.

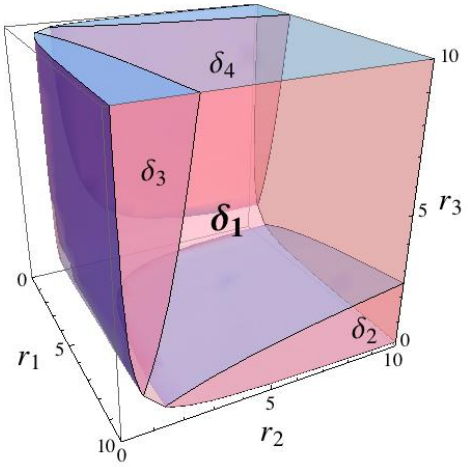

(a)

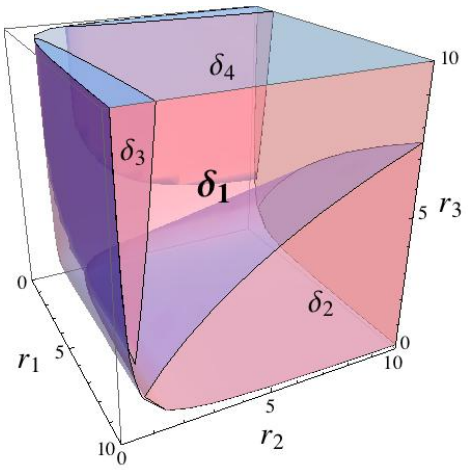

(b)

Figure 2.9: The range of validity for solutions rom Eq. (2.5.4) within the set of linearly independent states for a)$\eta_1 = \eta_2 = \eta_3 = 1/3$ and b)$\eta_1 = \eta_2 = 1/5$ and $\eta_3 = 3/5$. While δ_1 is a solution for the whole volume δ_2, δ_3 and δ_4 only occupy certain areas.

2.5.2 Three equal amplitudes

We start with the most basic case where all overlap amplitudes are equal, $s_1 = s_2 = s_3 \equiv s$, and the phase ϕ is arbitrary. Then the matrix C becomes

$$C = \begin{bmatrix} q_1 & se^{i\phi_{12}} & se^{-i\phi_{31}} \\ se^{-i\phi_{12}} & q_2 & se^{i\phi_{23}} \\ se^{i\phi_{31}} & se^{-i\phi_{23}} & q_3 \end{bmatrix}, \tag{2.5.9}$$

and its determinant

$$\det C = q_1 q_2 q_3 - s^2 \sum_i q_i + 2s^3 \cos\phi = 0. \tag{2.5.10}$$

Considering equal *a priori* probabilities, $\eta_i = \frac{1}{3}$, Eqs.(2.1.12) reduce to

$$\begin{aligned} q_1 &= \sqrt{\left(s^2 + \frac{\delta}{3}\right)}, \\ q_2 &= \sqrt{\left(s^2 + \frac{\delta}{3}\right)}, \\ q_3 &= \sqrt{\left(s^2 + \frac{\delta}{3}\right)}. \end{aligned} \tag{2.5.11}$$

Now that all failure probabilities are equal we define $q_1 = q_2 = q_3 \equiv q$. Replacing q_i by q in (2.5.10), the constraint immediately yields the equation

$$q^3 - 3s^2 q + 2s^3 \cos\phi = 0. \tag{2.5.12}$$

To determine q we use the parametrization $q = sq'$ and obtain the straightforward solutions

$$\begin{aligned} q'^{(0)} &= 2\cos\left(\frac{\pi-\phi}{3}\right), \\ q'^{(1)} &= -2\cos\left(\frac{\phi}{3}\right), \\ q'^{(2)} &= 2\cos\left(\frac{\pi+\phi}{3}\right). \end{aligned} \tag{2.5.13}$$

In Figure 2.10 we show the solutions q' as functions of the parameter ϕ.

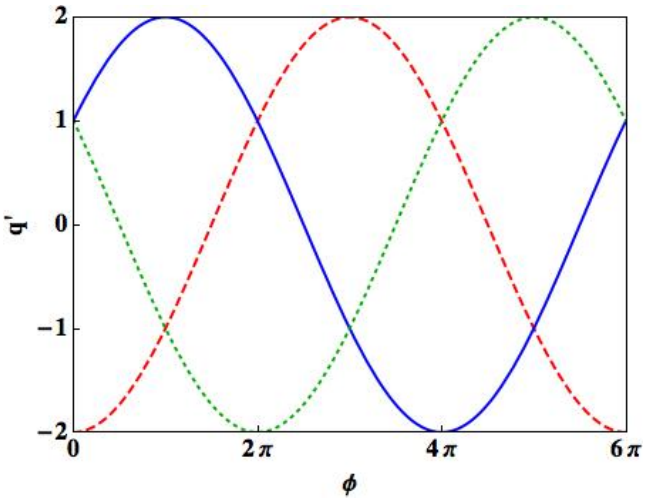

Figure 2.10: Solutions for cubic equation (2.5.12) as function of ϕ: $q'^{(0)}$ (solid line), $q'^{(1)}$ (dashed line), $q'^{(2)}$ (dotted line).

To choose the physical solutions, we will use the non-negativity of the sub-determinants of matrix C from Eqs. (2.1.9), which in this case are all

equal. They are:

$$\begin{aligned} \Delta_{kj} = q_k q_j - \langle\psi_k|\psi_j\rangle\langle\psi_j|\psi_k\rangle &= s^2 q^{'2} - s^2 \geq 0 \\ q^{'2} &\geq 1. \end{aligned} \tag{2.5.14}$$

We find that each of the three solutions is valid for a certain range of ϕ, specifically $2n\pi \leq \phi \leq 2\,(n+1)\,\pi$ with $n = 0, 1, 2$. The solutions are shown in Fig. 2.11 for $0 \leq \phi \leq 6\pi$.

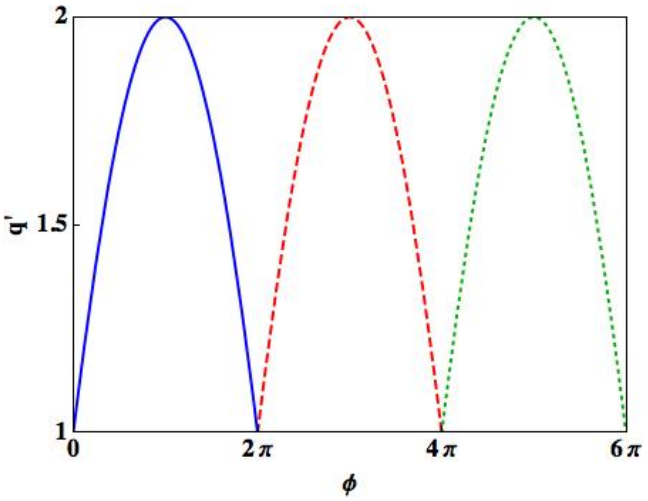

Figure 2.11: Solutions for cubic equation (2.5.12) as function of ϕ under the condition (2.5.14): $q'^{(0)}$ (solid line), $q'^{(1)}$ (dashed line), $q'^{(2)}$ (dotted line).

On the other hand, the individual failure probabilities also need to satisfy $0 \leq q \leq 1$. This condition, however, coincides in this case with the LI condition. If we have $\phi = \pi$ the possible maximum value for s would be $1/2$, for $\phi = \pi/2$ we need $s < 1/\sqrt{3}$ and so on. The total failure probability

is simply

$$Q = sq' = 2s\cos\left(\frac{\pi - \phi}{3}\right) \tag{2.5.15}$$

for $0 \leq \phi \leq 2\pi$ and can be seen in Figure 2.12.

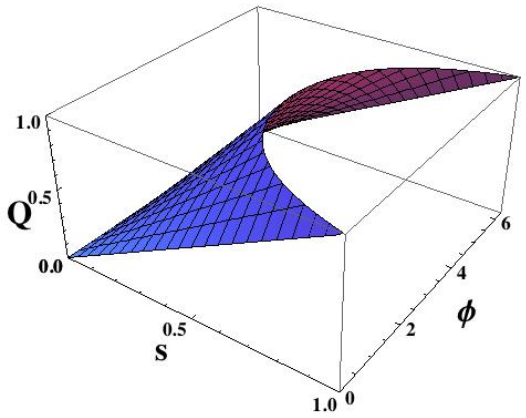

Figure 2.12: The total failure probability Q as a function of the amplitude s and the cocycle ϕ.

All scaled amplitudes are equal

Recall, that

$$\bar{s}_1 = \sqrt{\eta_2\eta_3}s_1, \tag{2.2.8}$$

and with obvious cyclic permutation of the indexes for the remaining overlaps.

We now have all scaled amplitudes equal

$$\bar{s}_1 = \bar{s}_2 = \bar{s}_3 \equiv \bar{s}. \tag{2.5.16}$$

Then the failure probabilities from Eq. (2.2.13) also are equal $\bar{q}_1 = \bar{q}_2 = \bar{q}_3 \equiv \bar{q}$ and reduce to

$$\bar{q} = \sqrt{\bar{s}^2 + \delta} \tag{2.5.17}$$

The constraint (Eq. (2.2.9) takes the form

$$\bar{q}^3 - 3\bar{s}^2\bar{q} + 2\bar{s}^3 \cos\phi = 0 \tag{2.5.18}$$

with solutions given by Eq. (2.5.13) with $\bar{q} = \bar{s}q'$. From the sub-determinants of the matrix C we get again

$$q'^2 \geq 1 \tag{2.5.19}$$

and Fig. 2.11 presents the solutions.

The question now is for what range the solutions are valid. For this, let us notice that we can express the relation in Eq. (2.5.16) in terms of the original parameters by the following ratios

$$\frac{s_1^2}{\eta_1} = \frac{s_2^2}{\eta_2} = \frac{s_3^2}{\eta_3}. \tag{2.5.20}$$

Consequently each of the above ratios must be separately equal to the same constant that we denote by c,

$$s_i^2 = c\eta_i, \tag{2.5.21}$$

for all i. Adding (2.5.21) for $i = 1, 2, 3$ and taking into account that $\eta_1 + \eta_2 + \eta_3 = 1$ we find $c = s_1^2 + s_2^2 + s_3^2$ and using this value of c in Eq. (2.5.21)

yields

$$\eta_i = \frac{s_i^2}{s_1^2 + s_2^2 + s_3^2}. \tag{2.5.22}$$

In other words, given an arbitrary set of overlaps, $\{s_1, s_2, s_3\}$, it is always possible to find a set of prior probabilities by the above prescription.

With Eqs. (2.5.16) and (2.5.22) the total failure probability is given by

$$Q = 3\ \bar{s}\ q' = \frac{3 s_1 s_2 s_3}{s_1^2 + s_2^2 + s_3^2}\ q' \tag{2.5.23}$$

We see that the case where all original amplitudes and priors are equal are contained in this solution as a special case. Hence, the scaling of the parameters allowed us to extend the range of validity.

2.5.3 Two equal amplitudes

The next case we consider is described by $s_1 = s_2 \equiv s$ and $s_3 \neq s$ in (2.0.1), and the phase ϕ is arbitrary. As we did in the last section (2.5.2) we are interested in the minimization of the total failure probability (2.1.3) under the constraint (2.1.7). Using the same procedure as before the equation we must solve is given by

$$q_1 q_2 q_3 + 2 s_1^2 s_2 \cos(\phi) - s_1^2 (q_1 + q_3) - q_2 s_2^2 = 0. \tag{2.5.24}$$

Having equal *a priori* probabilities $\eta_i = 1/3$, two of the failure probabilities are equal and one is different

$$\begin{aligned} q_1 &= \sqrt{\left(s_3^2 - \frac{1}{3\lambda}\right)}, \\ q_2 &= \sqrt{\left(s_3^2 - \frac{1}{3\lambda}\right)}, \\ q_3 &= \frac{\left(s_1^2 - \frac{1}{3\lambda}\right)}{\sqrt{\left(s_3^2 - \frac{1}{3\lambda}\right)}} \end{aligned} \tag{2.5.25}$$

and we also find

$$q_3 = \frac{s_1^2 - s_2^2 + q_1^2}{q_1}. \tag{2.5.26}$$

Therefore, the total failure probability takes the form

$$Q = \frac{3q_1^2 + s_1^2 - s_2^2}{3q_1}. \tag{2.5.27}$$

We define $q_1 = q_2 = q_i$ and $q_3 = q_j$ and correspondingly, $s_1 = s_i$ and $s_3 = s_j$. Replacing the solutions (2.5.25) and (2.5.26) in Eq. (2.5.24) we obtain a fourth order equation for the failure probability q_i

$$q_i^4 - q_i^2\left(2s_j^2 + s_i^2\right) + 2q_i s_i^2 s_j \cos\phi + s_j^2\left(s_j^2 - s_i^2\right) = 0,$$

or equivalently

$$q_i'^4 - q_i'^2\left(2 + \beta\right) + 2q_i'\beta\cos\phi + (1 - \beta) = 0 \tag{2.5.28}$$

where we have used the parametrization $q_i = s_j q_i'$ and the parameter $\beta = \frac{s_i^2}{s_j^2}$ has been defined. The quartic equation (2.5.28) can be solved using Ferrari's method. However the solutions are rather extensive and not very instructive. Therefore we present the four solutions for Eq. (2.5.28) graphically in Figure 2.13.

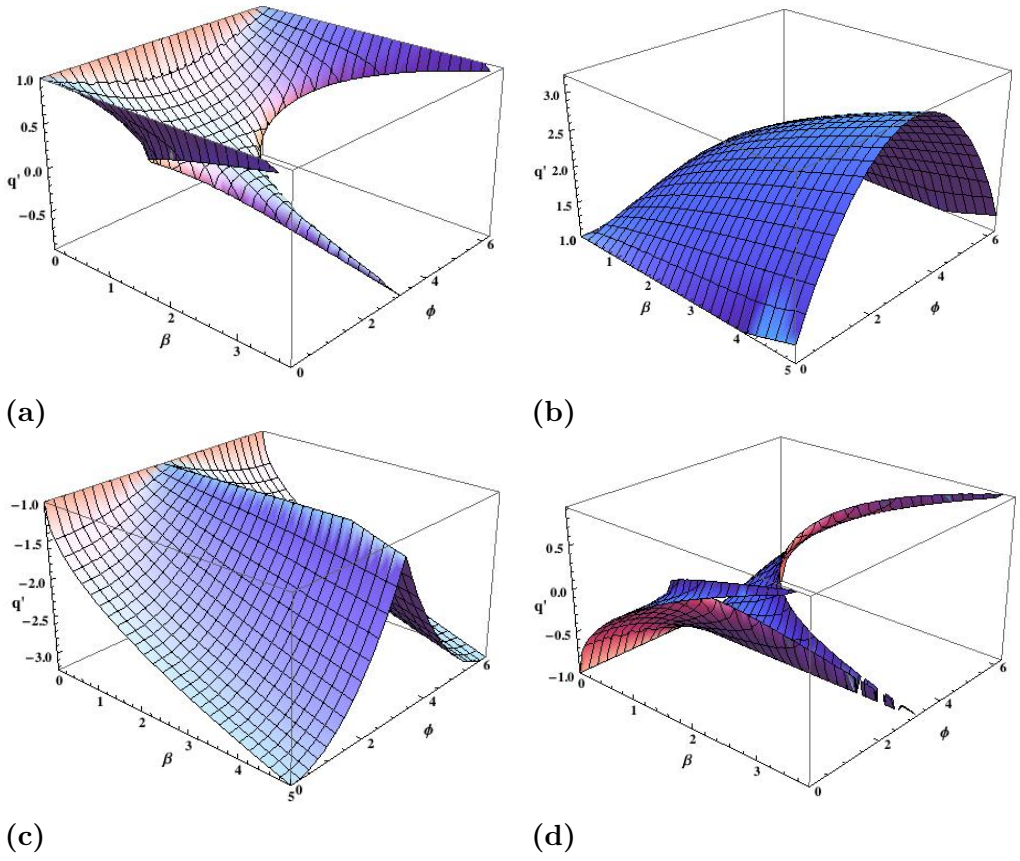

Figure 2.13: Solutions for quartic equation (2.5.28) as function of $\beta = \frac{s_1^2}{s_2^2}$ and the cocycle ϕ.

We can see that only three of the solutions have positive values. Using the fact that the sub-determinants of C have to be semidefinite positive, we

can choose the physical solutions. Again, we have

$$\begin{aligned} q_1^2 - s_2^2 &\geq 0, \\ q_i'^2 - 1 &\geq 0. \end{aligned} \tag{2.5.29}$$

For $0 < \phi < 2\pi$ Fig. 2.13b is the only solution that fulfills (2.5.29). However, for $\phi = 0$ Figures 2.13a and 2.13d are also valid solutions. In fact, solutions from Figures 2.13a and 2.13b are equal for $\phi = 0$ and reduce to $q_i' = 1$, while q_i' from Fig. 2.13d is $-1 + \sqrt{\beta}$. These agree with the solutions found in [53]. Solution $q_i' = 1$ will give the optimum for $\beta < 4$ and the overall failure probability in this case is

$$Q = \frac{s_1^2 + 2s_2^2}{3s_2} \tag{2.5.30}$$

with $q_1 = q_3 = s_2$ and $q_2 = s_1^2/s_2$. For $\beta \geq 4$ the second solution, $q_i' = -1 + \sqrt{\beta}$, will give the minimum value for the failure probability

$$Q = \frac{2}{3}(2s_1 - s_2) \tag{2.5.31}$$

with $q_1 = q_3 = s_1 - s_2$ and $q_2 = 2s_1$. In both cases $0 \leq q_i \leq 1$ is satisfied. For $0 < \phi < 2\pi$ the individual failure probabilities q_1 and q_2 as well as the total failure probability Q take a more complicated form. They can be seen in Fig. 2.14 for a value of $s_1 = 0.3$. In this case, the condition $0 \leq q_1 \leq 1$ is more restrictive than the L.I. condition. The difference in the valid range of values is illustrated by the dark area in Fig. 2.14a which reduces the upper limit of s_2. Here the condition $0 \leq q_2 \leq 1$ is already satisfied. However, for higher values of s_1 the condition for q_2 has to be considered separately

and will shrink the range of s_2 by increasing the lower limit. Furthermore, for q_1 the L.I. condition dominates for $s_2 < 0.5$ for higher values of s_1. As the range for valid s_2 is decreasing with increasing s_1, the overall failure probability Q also increases for fixed values of s_2.

2.5.4 Weighted equal probability measurement

The last case we consider is the weighted equal probability measurement (WEPM). In the case of equal probability measurement (EPM) the constraint is added that each state is determined with equal probability of success such that $p_1 = p_2 = p_3$ or conversely that the determination fails equally likely for each state $q_1 = q_2 = q_3$. This definition is widened to allow for cases where the failure probabilities are proportional to each other, i.e $\eta_1 q_1 = \eta_2 q_2 = \eta_3 q_3$. The latter case is what we call the weighted equal probability measurement (WEPM).

However we start with the conventional EPM which was first proposed by Chefles [46]. Then the constraint in Eq.(2.1.7) simplifies greatly to

$$q^3 - q\left(s_1^2 + s_2^2 + s_3^2\right) + 2s_1 s_2 s_3 \cos\phi = 0 \tag{2.5.32}$$

and the overall failure probability is just $Q_{EPM} = q$. While EPM (and WEPM), in general, is a suboptimal measurement Eldar [50] showed that EPM can be the optimal measurement for any set of state vectors with the right choice of a priori probabilities. For instance, in the case of m geometrically uniform states with a priori probabilities $\eta_i = 1/m$ EPM is always optimal. This is the case for $s_1 = s_2 = s_3 = s$ and equal a priori

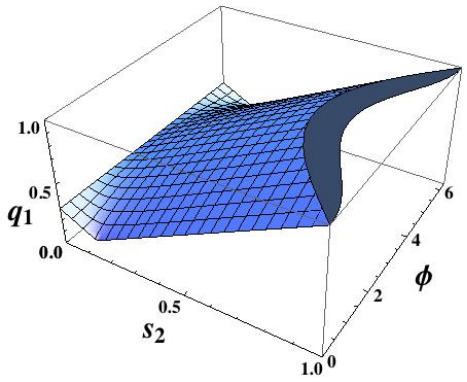

(a)

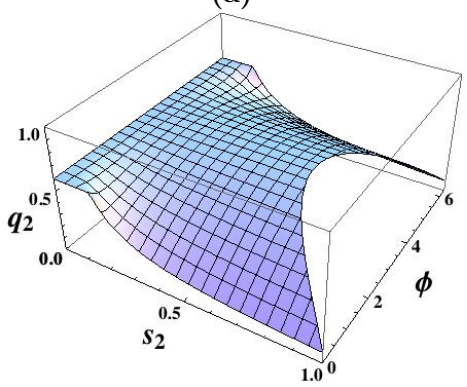

(b)

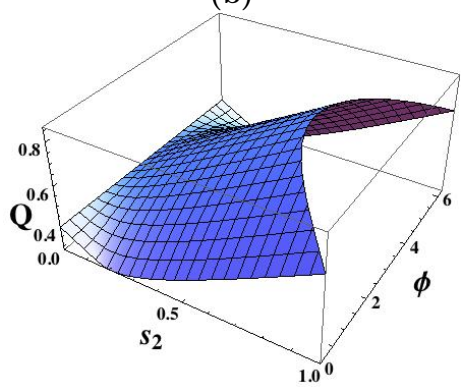

(c)

Figure 2.14: The individual failure probabilities q_1 (a) and q_2 (b) as well as the total failure probability Q (c) as a function of s_2 and ϕ for $s_1 = 0.3$. The dark area in (a) illustrates how the condition $0 \leq q_1 \leq 1$ reduces the range of valid values that was allowed by the L. I. condition.

probabilities, where Eq.(2.5.32) reduces to Eq. (2.5.12) with the already known solutions Eqs.(2.5.13).

Now, let us take a look at the case, where two amplitudes are equal, $s_1 = s_2$, and s_3 is different. The optimum measurement from Sec. 2.5.3 outperforms the EPM for equal a priori probabilities. If, however, the a priori probabilities are not equal, there are values of s_1, s_2 and ϕ where the EPM is equal to the optimal solution. This is the case if we choose $\eta_1 = \eta_2$ and $\eta_3 = 1 - 2\eta_1$ in the original problem. The constraint (2.1.7) will still lead to a quartic equation of the form of (2.5.28) and the solutions for the q' still hold. However, the parameter β as well as q_2 and the overall failure probability Q need to be adjusted such that

$$\beta = \frac{\eta_2 s_1^2}{\eta_1 s_2^2}, \tag{2.5.33}$$

$$q_2 = \frac{q_1^2\eta_1 + s_1^2\eta_2 - s_2^2\eta_1}{\eta_2 q_1}, \tag{2.5.34}$$

and the overall failure probability

$$Q = \frac{3q_1^2\eta_1 + s_1^2\eta_2 - s_2^2\eta_1}{q_1}. \tag{2.5.35}$$

In Fig. 2.15 Q and Q_{EPM} are plotted versus s_3 for a constant value of $s_1 = 0.3$ and $\phi = \pi/4$ and two different a priori probabilities, $\eta_1 = 2/5$ and $\eta_1 = 1/5$ respectively. While the two curves get close in both cases they only touch for $\eta_1 = 2/5$ (Fig. 2.15a). Here the difference $\Delta Q = Q_{EPM} - Q$ is *zero* for $s_3 \approx 0.41$ as can be seen from the insert in Fig. 2.15a. On the other hand, for $\eta_1 = 1/5$, ΔQ is positive for the whole range of s_3 (Fig.

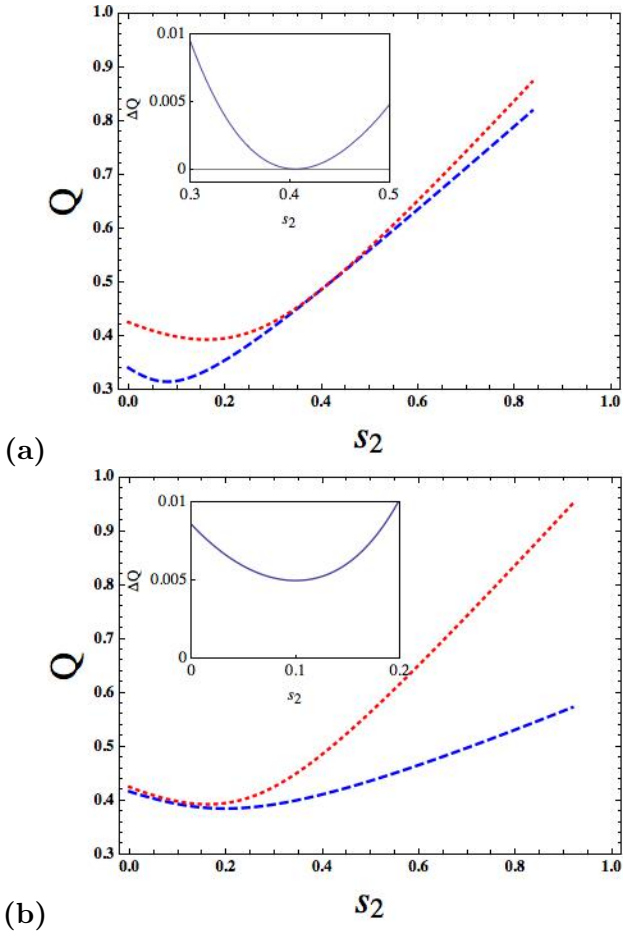

Figure 2.15: The optimum Q (dashed, blue) and the Q_{EPM} (dotted, red) for $s_1 = 0.3$, $\phi = \pi/4$ and two different a priori probabilities a) $\eta_1 = 2/5$ and b) $\eta_1 = 1/5$. The difference $\Delta Q = Q_{EPM} - Q$ versus s_3 is shown in the inserted graph.

2.15b). In this case the optimum Q again outperforms the Q_{EPM} over the whole range and considerably for ever larger values of s_3.

In general, the solutions to Eq. (2.5.32) take the following form

$$q = \frac{3^{\frac{1}{3}} r + \left(\sqrt{t^2 - 3r^3} - t\right)^{\frac{2}{3}}}{3^{\frac{2}{3}} \left(\sqrt{t^2 - 3r^3} - t\right)^{\frac{1}{3}}} \tag{2.5.36}$$

with

$$r = s_1^2 + s_2^2 + s_3^2 \quad \text{and} \quad t = 9 s_1 s_2 s_3 \cos\phi.$$

These agree with the results in [55]. As aforementioned for a certain choice of priori probabilities the EPM equals the optimal measurement. Using Eq. (2.1.11) those are

$$\begin{aligned} \eta_1 &= \frac{q^2 - s_1^2}{3q^2 - s_1^2 - s_2^2 - s_3^2}, \\ \eta_2 &= \frac{q^2 - s_2^2}{3q^2 - s_1^2 - s_2^2 - s_3^2}, \\ \eta_3 &= \frac{q^2 - s_3^2}{3q^2 - s_1^2 - s_2^2 - s_3^2}, \end{aligned} \tag{2.5.37}$$

where q is from Eq.(2.5.36).

The next example, we present, is a weighted equal-probability measurement or WEPM. In this case the individual failure probabilities are proportional to each other. Specifically, we have

$$\eta_1 q_1 = \eta_2 q_2 = \eta_3 q_3. \tag{2.5.38}$$

Thus, we can express two of the failure probabilities in terms of the third

$$q_2 = \frac{\eta_1}{\eta_2} q_1 \quad \text{and} \quad q_3 = \frac{\eta_1}{\eta_3} q_1. \tag{2.5.39}$$

Substituting Eq. (2.5.39) into Eq. (2.1.7) we have

$$q_1^3 - q_1 \left(s_1'^2 + s_2'^2 + s_3'^2 \right) + 2 s_1' s_2' s_3' \cos\phi = 0. \tag{2.5.40}$$

Here the overlaps s_1, s_2 and s_3 are replaced by their weighted counterparts s_1', s_2' and s_3'

$$\begin{aligned} s_1' &= \sqrt{\frac{\eta_2 \eta_3}{\eta_1^2}} s_1 \\ s_2' &= \sqrt{\frac{\eta_3}{\eta_1}} s_2 \\ s_3' &= \sqrt{\frac{\eta_2}{\eta_1}} s_3. \end{aligned} \tag{2.5.41}$$

The solution of Eq. (2.5.40) is given by Eq. (2.5.36) after replacing the overlaps with the weighted quantities. The overall failure probability is

$$Q_{WEPM} = 3 \eta_1 q_1. \tag{2.5.42}$$

Q_{WEPM} and the optimum Q are plotted for the special case where $s_1 = s_3$ in Fig. 2.16 for two values of the a priori probabilities, $\eta_1 = 2/5$ and $\eta_1 = 1/5$, and the fixed values of $s_1 = 0.3$ and $\phi = \pi/4$. In both graphs, the Q_{WEPM} follows the optimum Q more closely than the Q_{EPM} (Fig. 2.15). Q_{WEPM} is equal to the optimum Q at $s_2 \approx 0.21$ for $\eta_1 = 2/5$ (Fig. 2.16a) and

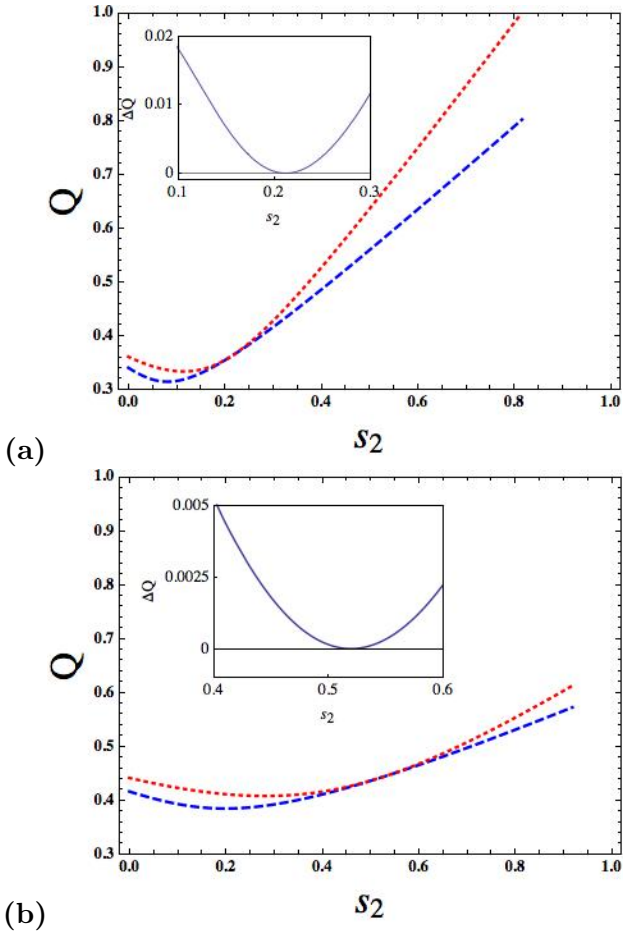

Figure 2.16: The optimum Q (dashed, blue) and the Q_{WEPM} (dotted, red) for $s_1 = 0.3$, $\phi = \pi/4$ and two different a priori probabilities a) $\eta_1 = 2/5$ and b) $\eta_1 = 1/5$. The difference $\Delta Q = Q_{WEPM} - Q$ versus s_2 is shown in the inserted graph.

at $s_2 \approx 0.52$ for $\eta_1 = 1/5$ (Fig. 2.16b). For the Q_{WEPM} to be equal to the optimal measurement we need to take into account the conditions Eq. (2.1.11). The individual failure probabilities can then be expressed in terms of the overlaps

$$q_2 = \frac{s_1^2}{s_2^2} q_1 \quad \text{and} \quad q_3 = \frac{s_1^2}{s_3^2} q_1. \tag{2.5.43}$$

Substituting Eq.(2.5.43) into Eq.(2.1.7) results in the following cubic equation:

$$q_1^3 - 3\gamma^2 q_1 + 2\gamma^3 \cos\phi = 0 \tag{2.5.44}$$

with the parameter

$$\gamma = \frac{s_2 s_3}{s_1}. \tag{2.5.45}$$

If we us the parametrization $q_1 = \gamma q'$, we will have

$$q'^3 - 3q' + 2\cos\phi = 0. \tag{2.5.46}$$

The solutions $q'^{(i)}$ with $i = 0, 1, 2$ are given by Eq. (2.5.13) for the appropriate range of ϕ. Using the a priori probabilities

$$\begin{aligned} \eta_1 &= \frac{s_1^2}{s_1^2 + s_2^2 + s_3^2}, \\ \eta_2 &= \frac{s_2^2}{s_1^2 + s_2^2 + s_3^2}, \\ \eta_3 &= \frac{s_3^2}{s_1^2 + s_2^2 + s_3^2}, \end{aligned} \tag{2.5.47}$$

the total failure probability takes the following form

$$Q = \frac{3s_1s_2s_3}{s_1^2 + s_2^2 + s_3^2} q'^{(i)}. \tag{2.5.48}$$

Note, the case when the WEPM is optimal coincides with the case where all scaled overlaps are equal $\bar{s}_1 = \bar{s}_2 = \bar{s}_3 \equiv \bar{s}$.

Obviously, using scaled parameters is tantamount to using weighted parameters. Let us illustrate this point by presenting a case of equal scaled failure probabilities. For example using Scaling A we set all scaled failure probabilities equal $\tilde{q}_1 = \tilde{q}_2 = \tilde{q}_3 = \tilde{q}$. Then the constraint in Eq. (2.2.3) becomes

$$\tilde{q}^3 - 3\tilde{q} + 2\cos\phi = 0. \tag{2.5.49}$$

Again, the solutions are the $q'^{(i)}$ from Eq. (2.5.13). After re-substituting the scaled parameters by the original ones the total failure probability is

$$Q_{WEPM} = 2\left(\frac{s_2s_3}{s_1}\ \eta_1 + \frac{s_1s_3}{s_2}\ \eta_2 + \frac{s_1s_2}{s_3}\ \eta_3\right)\cos\left(\frac{\pi - \phi}{3}\right) \tag{2.5.50}$$

where the $q'^{(1)}$ solution was used as an example. Eq. (2.5.50) will be optimal if the a priori probabilities are chosen according to Eq. (2.5.47). Indeed, Eq. (2.5.50) gives the same result as Eq. (2.5.48).

In conclusion, the WEPM always performs better than the EPM. The above result Eqs. (2.5.48) and (2.5.50) cover a broad range of values for arbitrary overlap amplitudes and arbitrary cocycle ϕ. The Q_{WEPM} is close to the optimal Q in most cases and it is optimal if the a priori probabilities are adjusted according to Eq. (2.5.47).

2.6 POVM elements for three non-orthogonal states

We present the POVM elements for three non-orthogonal states in terms of the a priori probabilities η_i and the states $|\psi_i\rangle$ with $i = 1, 2, 3$. Note, that the no-error condition requires that the direction of the components of Π_i is perpendicular to the plane spanned by the states $|\psi_j\rangle$ and $|\psi_k\rangle$ with $i \neq j$ and $i \neq k$. Or equivalently, Π_i has no component in the direction of $|\psi_j\rangle$ and $|\psi_k\rangle$ with $i \neq j$ and $i \neq k$. This also illustrates the necessity of the states to be linearly independent. If they were not there would be no way to find an operator Π_i that .... On the other hand, Π_i is not a full projector but only proportional to one because of the non-orthogonality of the states $|\psi_i\rangle$.

Let us start by writing down the state of the system as sum of the individual density matrices

$$\rho = \rho_1 + \rho_2 + \rho_3, \tag{2.6.1}$$

where

$$\begin{aligned} \rho_1 &= \eta_1 |\psi_1\rangle\langle\psi_1|, \\ \rho_2 &= \eta_2 |\psi_2\rangle\langle\psi_2|, \\ \rho_3 &= \eta_3 |\psi_3\rangle\langle\psi_3|. \end{aligned} \tag{2.6.2}$$

Now we multiply Eq. (2.6.1) from left and right with $\frac{1}{\sqrt{\rho}}$

$$\frac{1}{\sqrt{\rho}}\rho\frac{1}{\sqrt{\rho}} = \frac{1}{\sqrt{\rho}}\rho_1\frac{1}{\sqrt{\rho}} + \frac{1}{\sqrt{\rho}}\rho_2\frac{1}{\sqrt{\rho}} + \frac{1}{\sqrt{\rho}}\rho_3\frac{1}{\sqrt{\rho}}, \tag{2.6.3}$$

which gives us the following resolution of the identity

$$I = \tilde{\rho}_1 + \tilde{\rho}_2 + \tilde{\rho}_3 \tag{2.6.4}$$

where

$$\tilde{\rho}_i = \frac{1}{\sqrt{\rho}} \rho_i \frac{1}{\sqrt{\rho}} \tag{2.6.5}$$

and $i = 1, 2, 3$. Since we deal with pure states the original density matrices ρ_i are rank-1 operators. Therefore the new density matrices $\tilde{\rho}_i$ are also rank-1 and are orthogonal to each other. We can write them as

$$\tilde{\rho}_i = |i\rangle\langle i|. \tag{2.6.6}$$

Now, if we transform the POVM elements Π_i that discriminate the state $|\psi_i\rangle$ correctly as well we obtain

$$\tilde{\Pi}_i = \sqrt{\rho}\ \Pi_i \sqrt{\rho} \tag{2.6.7}$$

for $i = 1, 2, 3$. Clearly, these new operators $\tilde{\Pi}_i$ are simply proportional to the projectors onto the space of the new density matrices $\tilde{\rho}_i$ and we have

$$\tilde{\Pi}_i = c_i |i\rangle\langle i| = c_i \frac{1}{\sqrt{\rho}} \rho_i \frac{1}{\sqrt{\rho}}. \tag{2.6.8}$$

where c_i are some positive numbers, yet to be determined. Hence, after transforming them back the original operators Π_i take the following form

$$\Pi_i = \frac{1}{\sqrt{\rho}} \tilde{\Pi}_i \frac{1}{\sqrt{\rho}} = c_i \rho^{-1} \rho_i \rho^{-1}. \tag{2.6.9}$$

The POVM element for the inconclusive outcome is

$$\Pi_0 = 1 - \sum_i c_i \rho^{-1} \rho_i \rho^{-1}. \tag{2.6.10}$$

As we can see, minimizing the inconclusive outcome depends now on the new parameters c_i. We notice that,

$$\mathrm{Tr}\ (\tilde{\rho}_i\ \tilde{\Pi}_i) = \mathrm{Tr}\ (\frac{1}{\sqrt{\rho}}\ \rho_i\ \frac{1}{\sqrt{\rho}}\ \sqrt{\rho}\ \Pi_i \sqrt{\rho}) = \mathrm{Tr}\ (\rho_i\ \Pi_i). \tag{2.6.11}$$

Consequently, we can identify the c_i as the individual failure probabilities weighted by the a priori probabilities such as

$$c_i = \eta_i p_i. \tag{2.6.12}$$

Using, the fact that Π_0 is a positive operator and therefore, $\det \Pi_0 \geq 0$, we have

$$\begin{aligned} &\eta_1\eta_2\eta_3 \left(1 - s_1^2 - s_2^2 - s_3^2 + 2 s_1 s_2 s_3 \cos\phi\right) - c_1 c_2 c_3 + c_1 c_2 \eta_3 + c_1 c_3 \eta_2 + c_2 c_3 \eta_1 \\ &- c_1 \eta_2 \eta_3 \left(1 - s_1^2\right) - c_2 \eta_1 \eta_3 \left(1 - s_2^2\right) - c_3 \eta_1 \eta_2 \left(1 - s_3^2\right) \geq 0. \end{aligned} \tag{2.6.13}$$

If the parameters c_i are replaced by $\eta_i p_i$ and $q_i = 1 - p_i$, Eq. (2.6.13) becomes Eq. (2.1.7). Hence, the optimization of c_i is equivalent to minimizing q_i. The optimization problem has the form already discussed in Sec. 2.1 with solutions to the special cases in Sec. 2.5.

Finally, we can write the POVM elements for the general case explicitly

as

$$
\begin{aligned}
\Pi_1 &= p_1 \begin{bmatrix} 1 & \frac{-s_3}{\sqrt{1-s_3^2}} & \frac{s_1 s_3 e^{i\phi}-s_2}{\sqrt{1-s_3^2}\sqrt{G}} \\ \frac{-s_3}{\sqrt{1-s_3^2}} & \frac{s_3}{1-s_3^2} & \frac{s_3\left(s_2-s_1 s_3 e^{i\phi}\right)}{\left(1-s_3^2\right)\sqrt{G}} \\ \frac{s_1 s_3 e^{-i\phi}-s_2}{\sqrt{1-s_3^2}\sqrt{G}} & \frac{s_3\left(s_2-s_1 s_3 e^{-i\phi}\right)}{\left(1-s_3^2\right)\sqrt{G}} & \frac{s_2^2+s_1^2 s_3^2-2s_1 s_2 s_3\cos\phi}{\left(1-s_3^2\right)G} \end{bmatrix} \\
\Pi_2 &= p_2 \begin{bmatrix} 0 & 0 & 0 \\ 0 & \frac{1}{1-s_3^2} & \frac{s_2 s_3-s_1 e^{i\phi}}{\left(1-s_3^2\right)\sqrt{G}} \\ 0 & \frac{s_2 s_3-s_1 e^{-i\phi}}{\left(1-s_3^2\right)\sqrt{G}} & \frac{s_1^2+s_2^2 s_3^2-2s_1 s_2 s_3\cos\phi}{\left(1-s_3^2\right)G} \end{bmatrix} \\
\Pi_3 &= p_3 \begin{bmatrix} 0 & 0 & 0 \\ 0 & 0 & 0 \\ 0 & 0 & \frac{\left(1-s_3^2\right)}{G} \end{bmatrix} \\
\Pi_0 &= \begin{bmatrix} 1-p_1 & \frac{p_1 s_3}{\sqrt{1-s_3^2}} & \frac{p_1\left(s_2-s_1 s_3 e^{i\phi}\right)}{\sqrt{1-s_3^2}\sqrt{G}} \\ \frac{p_1 s_3}{\sqrt{1-s_3^2}} & 1-\frac{p_2+p_1 s_3^2}{1-s_3^2} & \frac{\left(p_2+p_1 s_3^2\right)s_1 e^{i\phi}-(p_1+p_2)s_2 s_3}{\left(1-s_3^2\right)\sqrt{G}} \\ \frac{p_1\left(s_2-s_1 s_3 e^{-i\phi}\right)}{\sqrt{1-s_3^2}\sqrt{G}} & \frac{\left(p_2+p_1 s_3^2\right)s_1 e^{-i\phi}-(p_1+p_2)s_2 s_3}{\left(1-s_3^2\right)\sqrt{G}} & 1+\frac{p_1+p_2}{1-s_3^2}-\frac{p_1\left(1-s_1^2\right)+p_2\left(1-s_2^2\right)+p_3\left(1-s_3^2\right)}{G} \end{bmatrix}
\end{aligned}
\tag{2.6.14}
$$

and $G = 1 - s_1^2 - s_2^2 - s_3^2 + 2s_1 s_2 s_3 \cos\phi$.

Chapter 3

Identification of unknown pure states

3.1 Identification of unknown pure states as a case of mixed state discrimination

Let the states $|i\rangle_n$ denote an orthonormal basis of the n-th qudit in the d-dimensional Hilbert space. Then the identity operator in the space of the n-th qudit is

$$I_n = \sum_{i=0}^{d-1} |i\rangle_{nn}\langle i| \quad (n = 0, 1, \ldots, N). \tag{3.1.1}$$

Suppose we are given an unknown, pure, d-dimensional quantum state $|\psi\rangle$. This state is guaranteed to be one out of a set of pure quantum states $\{|\psi_1\rangle, |\psi_2\rangle, \ldots |\psi_N\rangle\}$. The states of the set are also unknown. The state $|\psi\rangle$ is called the probe or data state and has the index 0. The set of states is provided as reference and is labelled by indices 1 through N. In the case where the probe matches the n-th reference qudit the state of the whole

$N+1$ system is given by

$$|\Psi_n\rangle = |\psi_n\rangle_0 |\psi_1\rangle_1 \ldots |\psi_N\rangle_N. \tag{3.1.2}$$

These N states have equal a priori probability $1/N$.

Since the reference states are unknown the state identification strategy must be independent of said states. Therefore the task is to find a measurement that is optimal on average. To express our lack of classical knowledge we take the average over all possible qudit states

$$\rho_n = \{|\Psi_n\rangle\langle\Psi_n|\}_{ave}. \tag{3.1.3}$$

The state ρ_n is independent of a particular orthonormal basis. However it spans the symmetric subspace of the probe and the n-th qudit and is uniformly distributed over the remainder of the $N-1$ reference states. From symmetry considerations it then follows that, for the case when the probe matches the n-th reference state, the total $(N+1)$-qudit system is characterized by the average density operator

$$\rho_n = \frac{2}{(d+1)d^N}\, P_{0,n}^{sym} \bigotimes_{\substack{i=1 \\ i\neq n}}^{N} I_i \qquad (n = 1, \ldots, N) \tag{3.1.4}$$

where I_i is given by Eq. (3.1.1) and the operator $P_{0,n}^{sym}$ is the projector onto the symmetric part of the two-qudit subspace jointly spanned by the eigenstates of the probe qudit and the n-th reference qudit. The two-qudit symmetric subspace has the dimension $d(d+1)/2$. Together with the $N-1$

reference states, each d-dimensional, this leads to a normalization factor of $2/(d+1)d^N$. The projector onto the two-qudit symmetric subspace is

$$P_{0,n}^{sym} = \sum_{i=0}^{d-1} |i\rangle_0|i\rangle_n\langle i|_0\langle i|_n + \sum_{j=1}^{d-1}\sum_{i=0}^{j-1} \frac{|i\rangle_0|j\rangle_n + |j\rangle_0|i\rangle_n}{\sqrt{2}} \frac{\langle i|_0\langle j|_n + \langle j|_0\langle i|_n}{\sqrt{2}}. \tag{3.1.5}$$

$P_{0,n}^{sym}$ together with $P_{0,n}^{as}$, the projector onto the antisymmetric subspace of two qudits, sum to $P_{0,n}$, the projector onto the two-qudit subspace of dimension d^2 jointly spanned by the eigenstates of the probe qudit and the n-th reference qudit with

$$P_{0,n}^{as} = \sum_{j=1}^{d-1}\sum_{i=0}^{j-1} \frac{|i\rangle_0|j\rangle_n - |j\rangle_0|i\rangle_n}{\sqrt{2}} \frac{\langle i|_0\langle j|_n - \langle j|_0\langle i|_n}{\sqrt{2}} \tag{3.1.6}$$

and

$$P_{0,n} = P_{0,n}^{sym} + P_{0,n}^{as} = I_0 \otimes I_n \qquad (n \neq 0). \tag{3.1.7}$$

In analogy to the treatment in [73, 77, 74, 75] the state identification problem of N unknown, pure states is now reduced to discriminating between the N mixed states represented by the density matrices in Eq. (3.1.4).

3.2 Unambiguous identification of N unknown, pure qudit states

In order to unambiguously indentify the probe qudit with one of the N linearly independent reference states, we have to discriminate between the N density matrices ρ_n given by

$$\rho_n = \frac{2}{(d+1)d^N} P_{0,n}^{sym} \bigotimes_{\substack{i=1 \\ i\neq n}}^{N} I_i \qquad (n = 1, \ldots, N) \tag{3.1.4}$$

To perform this task we require $(N+1)$ positive detection operators $\Pi_1, \ldots \Pi_N$ and Π_0 whose sum is the identity

$$\sum_{n=1}^{N} \Pi_n + \Pi_0 = I \equiv I_0 \otimes I_1 \otimes \ldots \otimes I_N. \tag{3.2.1}$$

The detection operators are defined in such a way that $\mathrm{Tr}(\rho_n \Pi_n)$ is the probability of successfully identifying the density operator as ρ_n, while $\mathrm{Tr}(\rho_n \Pi_m)$ $(m \neq n)$ describes the probability to infer an erroneous result and $\mathrm{Tr}(\rho_n \Pi_0)$ is the probability that the measurement result is inconclusive, i. e. that the discrimination attempt fails to give a definite answer [93, 94]. It is a requirement for unambiguous discrimination that $\mathrm{Tr}(\rho_n \Pi_m) = 0$ for $m \neq n$, and from the condition for the positivity of the operators ρ_n and Π_m it follows that this requirement can only be met when

$$\rho_n \Pi_m = 0 \qquad \text{if} \quad m \neq n \tag{3.2.2}$$

[93, 94]. Here we are considering that N mixed states occur with equal prior probability, given by $1/N$, so that the overall success probability of the discrimination measurement takes the form

$$P_{succ} = \frac{1}{N} \sum_{n=1}^{N} \mathrm{Tr}(\rho_{\mathrm{n}} \Pi_{\mathrm{n}}). \tag{3.2.3}$$

For the optimum measurement, we need to find the detection operators Π_n that maximize the success probability P_{succ} under the constraint of non-negativity of the eigenvalues of the operator $\Pi_0 = I - \sum_{n=1}^{N} \Pi_n$.

3.2.1 Detection Operators for three unknown ququartz states

Before we derive the general structure of the detection operators, let's consider first only three density operators ρ_1, ρ_2 and ρ_3 given by Eq. (3.1.4) with $d = 4$ and $N = 3$. This is the unambiguous identification of three unknown, pure ququartz states. We proceed along the lines of unambiguous discrimination of mixed quantum states [58, 62, 59] and follow a similar procedure as for the case of d unknown, pure qudits [81].

Let us start with Π_1 which discriminates the state ρ_1. As we know, in unambiguous state discrimination strategy errors are not allowed and therefore our Π_1 is required to fulfill the following relation

$$\Pi_1 \rho_2 = \Pi_1 \rho_3 = 0. \tag{3.2.4}$$

Obviously, Π_1 meets this requirement when its support is orthogonal to the supports of ρ_2 and ρ_3, or, rephrased, if it belongs simultaneously to the

kernel of ρ_2 and to the kernel of ρ_3. From Eqs. (3.1.7) and (3.1.4) we can write the projectors onto these two kernels as

$$P_{K_2} = P^{as}_{0,2} \otimes I_1 \otimes I_3 \qquad \text{and} \qquad P_{K_3} = P^{as}_{0,3} \otimes I_1 \otimes I_2. \tag{3.2.5}$$

Since I_1 is common to both, the projector P_{Π_1} onto the support of Π_1 can be written as

$$P_{\Pi_1} = I_1 \otimes P'_{\Pi_1}, \tag{3.2.6}$$

where P'_{Π_1} projects onto the subspace spanned by all states $|\varphi\rangle$ that are linear combinations of the eigenstates of the operator $P^{as}_{0,2} \otimes I_3$, on the one hand, and also linear combinations of the eigenstates of the operator $P^{as}_{0,3} \otimes I_2$, on the other hand. We denote the corresponding eigenstates by $|a_l\rangle$ for $P^{as}_{0,2} \otimes I_3$, and by $|b_l\rangle$ for $P^{as}_{0,3} \otimes I_2$,

$$2^{-1/2}(|i\rangle_0|j\rangle_2 - |i\rangle_2|j\rangle_0)\,|k\rangle_3 \;\;\rightarrow\;\; |a_l\rangle, \tag{3.2.7}$$

$$2^{-1/2}(|i\rangle_0|j\rangle_3 - |i\rangle_3|j\rangle_0)\,|k\rangle_2 \;\;\rightarrow\;\; |b_l\rangle, \tag{3.2.8}$$

with $i < j$ and $i, j, k = 0, 1, 2, 3$, where $l = 1, \ldots, 24$ labels the twenty four triples $\{i, j, k\}$ as follows

l	$\{i,j,k\}$	l	$\{i,j,k\}$	l	$\{i,j,k\}$	l	$\{i,j,k\}$
1	{1,2,0}	4	{1,3,0}	7	{2,3,0}	10	{2,3,1}
2	{0,2,1}	5	{0,3,1}	8	{0,3,2}	11	{1,3,2}
3	{0,1,2}	6	{0,1,3}	9	{0,2,3}	12	{1,2,3}

and for $l \geq 13$ either $i = k$ or $j = k$. For determining $|\varphi\rangle$ we put

$$|\varphi\rangle = \sum_{l=1}^{24} a_l |a_l\rangle = \sum_{l=1}^{24} b_l |b_l\rangle, \tag{3.2.9}$$

where a_l and b_l are some complex coefficients. Since $a_l = \sum_{l'} b_{l'} \langle a_l | b_{l'} \rangle$ and $b_l \sum_{l'} a_{l'} \langle b_l | a_{l'} \rangle$, we obtain

$$b_l = \sum_{l''=1}^{24} b_{l''} \left(\sum_{l'=1}^{24} \langle b_l | a_{l'} \rangle \langle a_{l'} | b_{l''} \rangle \right) = \sum_{l''=1}^{24} b_{l''} \, B_{ll''}. \tag{3.2.10}$$

Using Eqs. (3.2.7) and (3.2.8) we have the following values for $B_{ll''}$

l'' \ l	1	2	3
1	$\frac{1}{2}$	$-\frac{1}{4}$	$\frac{1}{4}$
2	$-\frac{1}{4}$	$\frac{1}{2}$	$-\frac{1}{4}$
3	$\frac{1}{4}$	$-\frac{1}{4}$	$\frac{1}{2}$

and similarly if we exchange $\{1, 2, 3\}$ with $\{4, 5, 6\}$, $\{7, 8, 9\}$ or $\{10, 11, 12\}$. Furthermore $B_{ll''} = 1/4$ if $l = l''$and $l, l'' \geq 13$ and all other $B_{ll''} = 0$.

The only non-trivial solution of the system of equations given by Eq. (3.2.10) reads $b_l = -c$ for $l \in \{1, 3, 4, 6, 7, 9, 10, 12\}$ and $b_l = c$ for $l \in \{2, 5, 8, 11\}$ with c being an arbitrary constant, while $b_l = 0$ if $l \geq 13$. Upon inserting these values into Eq. (3.2.9) and applying Eq. (3.2.8) we arrive at the four eigenstates $|\varphi_{1q}(3, 4)\rangle$ of P'_{Π_1} with $q = 1, 2, 3, 4$ representing one set of excitation numbers $\{i, j, k\}$ and their permutations. Similarly the projectors onto the support of the other two detection operators can be

represented as $P_{\Pi_n} = I_n \otimes P'_{\Pi_n}$ with $n = 2, 3$.

Finally the four eigenstates $|\varphi_{nq}(3,4)\rangle$ for $n = 1, 2, 3$ have the following form

$$|\varphi_{n1}(3,4)\rangle = \frac{(-1)^n}{\sqrt{3}}\,(-b_1 + b_2 - b_3) \tag{3.2.11}$$

$$|\varphi_{n2}(3,4)\rangle = \frac{(-1)^n}{\sqrt{3}}\,(-b_4 + b_5 - b_6) \tag{3.2.12}$$

$$|\varphi_{n3}(3,4)\rangle = \frac{(-1)^n}{\sqrt{3}}\,(-b_7 + b_8 - b_9) \tag{3.2.13}$$

$$|\varphi_{n4}(3,4)\rangle = \frac{(-1)^n}{\sqrt{3}}\,(-b_{10} + b_{11} - b_{12})\,. \tag{3.2.14}$$

The $|\varphi_{nq}(3,4)\rangle$ are tripartite states. The indices labeling the states b_l are $(0,3,2)$, $(0,3,1)$ and $(0,2,1)$ for $n = 1, 2, 3$, respectively.

In $|\varphi_{nq}(N,d)\rangle$ the index n refers to the fact that it is the eigenstate of this projector and the argument $N = 3$ to the fact that we are discriminating three states and $d = 4$ to the fact that we are dealing with the ququartz case. The eigenstates are totally antisymmetric states of three qudits. There are $\binom{4}{3}$ totally antisymmetric states $|\varphi_{nq}(N,d)\rangle$ spanning the antisymmetric subspace of N states in d dimensions. The index q numbers those states.

Thus we obtain for $n = 1, 2, 3$

$$P_{\Pi_n} = I_n \otimes \sum_{q=1}^{4} |\varphi_{nq}(3,4)\rangle\langle\varphi_{nq}(3,4)| = \sum_{k=0}^{3}\sum_{q=1}^{4} |\pi_{nq}^{(k)}\rangle\langle\pi_{nq}^{(k)}|, \tag{3.2.15}$$

where

$$|\pi_{nq}^{(k)}\rangle = |k\rangle_n \otimes \sum_{q=1}^{4} |\varphi_{nq}(3,4)\rangle \quad (k = 0, 1, 2, 3). \tag{3.2.16}$$

Since the states $|\pi_{nq}^{(k)}\rangle$ are orthonormal basis states of the support of Π_n, it follows that Π_n can be represented as

$$\Pi_n = \sum_{k,k'=0}^{3} \sum_{q=1}^{4} \alpha_n^{(k,k')} |\pi_{nq}^{(k)}\rangle\langle\pi_{nq}^{(k')}| \quad (n = 1, 2, 3), \tag{3.2.17}$$

where the coefficients $\alpha_n^{(k,k')}$ are some complex constants that have to follow the positivity condition for the detection operators.

3.2.2 Detection Operators for N unknown qudit states

Now we return to the general caseof identifying N qudit states given by Eq. (3.1.4) unambiguously. By the same reasoning as for the three states in $d = 4$ dimensions, the projector onto the support of the detection operators Π_n is of the form

$$P_{\Pi_n} = I_n \otimes P'_{\Pi_n} \tag{3.2.18}$$

Here P'_{Π_n} is the projector onto the subspace spanned by all states that can simultaneously written as linear combinations of the eigenstates of any of the operators $P_{0,m}^{as} \bigotimes_i I_i$, where $m \neq n$ and $i \neq m, n$. Generalizing Eq. (3.2.15), the projector is

$$P_{\Pi_n} = I_n \otimes |\varphi_{nq}(N, d)\rangle\langle\varphi_{nq}(N, d)| = \sum_{k=0}^{d-1} \sum_{q=1}^{\binom{d}{N}} |\pi_{nq}^{(k)}\rangle\langle\pi_{nq}^{(k)}| \tag{3.2.19}$$

with

$$|\pi_{nq}^{(k)}\rangle = |k\rangle_n \otimes |\varphi_{nq}(N, d)\rangle \quad (k = 0, \ldots, d-1) \tag{3.2.20}$$

where

$$|\varphi_{nq}\,(N,d)\rangle = \frac{(-1)^n}{\sqrt{n!}} \sum_{\sigma_q} sgn(\sigma_q) \bigotimes_{\substack{j=0 \\ j\neq n}}^{N} |\sigma_{qj}\rangle_j. \tag{3.2.21}$$

The $|\varphi_{nq}(N,d)\rangle$ are the completely antisymmetric states of N states in a d-dimensional Hilbert space. σ_q refers to a specific selection of $N \leq d$ excitation numbers out of the set of all d excitation numbers $\sigma_j = 0, 1, \ldots, d-1$. The n-th reference qudit is omitted from the total system of $N+1$ qudits resulting in a N qudit system and the sum in Eq. (3.2.21) is taken over all $N!$ permutations σ_q distributing those excitation numbers over the system of the remaining N qudits. The latter are written in fixed order and $\mathrm{sgn}(\sigma_q)$ denotes the sign of the permutation. There are $\binom{d}{N}$ distinct sets σ_q.

Since each σ_q contains a different subset of excitation numbers, we can immediately write

$$\langle \varphi_{nq}\,(N,d)\,|\varphi_{nq'}\,(N,d)\rangle = \delta_{q,q'} \tag{3.2.22}$$

Together with $\langle \pi_{nq}^{(k)} | \pi_{nq}^{(k')} \rangle = \delta_{k,k'}$ we can represent the detection operators as

$$\Pi_n = \sum_{k,k'=0}^{d-1} \sum_{q=1}^{\binom{d}{N}} \alpha_n^{(k,k')} |\pi_{nq}^{(k)}\rangle\langle\pi_{nq}^{(k')}| \quad (n = 1, \ldots, N), \tag{3.2.23}$$

where $\alpha_n^{(k,k')}$ are complex coefficients, that have to be determined such that $\Pi_n \geq 0$ and $\Pi_0 = I - \sum_{n=1}^{n_d} \Pi_n \geq 0$ hold.

This set of detection operators will never give an erroneous result as is

required of an unambiguous discrimination (Eq. (3.2.2))

$$\begin{array}{lll} \rho_n & |\pi_{mq}^{(k)}\rangle & \propto \\ & |k\rangle_n & \sum_{\sigma_q} sgn(\sigma_q) \bigotimes_{\substack{j=1 \\ j\neq n,m}}^{N} |\sigma_{qj}\rangle_j P_{0,m}^{sym} |\sigma_{q0}\rangle_0 |\sigma_{qm}\rangle_m = 0 \end{array} \tag{3.2.24}$$

where the terms $P_{0,m}^{sym}|i\rangle_0|j\rangle_m$ and $P_{0,m}^{sym}|j\rangle_0|i\rangle_m$ cancel each other due to the opposite sign of the respective permutation. Eq. (3.2.19) is, therefore, sufficient for P_{Π_n} to be a projector onto the support of the detection operator Π_n.

From [80] the necessary condition for the Π_n (Eq. (3.2.23)) to be unambiguous programmable discriminator for N states is that the support of $\mathrm{Tr_n}(\Pi_\mathrm{n})$ lies in the antisymmetric subspace of N qudits, where $\mathrm{Tr_n}$ is the partial trace over the n-th subsystem. With

$$\mathrm{Tr_n}(\Pi_\mathrm{n}) = \sum_{k,k'=0}^{d-1} \sum_{q=1}^{\binom{d}{N}} \alpha_n^{(k,k')} |\varphi_{nq}(N,d)\rangle\langle\varphi_{nq}(N,d)| \tag{3.2.25}$$

this requirement is also met.

We conclude this section with some useful relationships between the N qudit states $|\pi_{nq}^{(k)}\rangle$. First, if $m = n$ we have

$$\langle\pi_{nq}^{(k)}|\pi_{mq'}^{(k')}\rangle = \delta_{k,k'}\delta_{q,q'}. \tag{3.2.26}$$

If $m \neq n$ the inner product $\langle \pi^{(k)}_{nq} | \pi^{(k')}_{mq'} \rangle$ takes the form

$$\frac{(-1)^{(n+m)}}{N!} \sum_{\substack{\sigma \\ \sigma'}} \mathrm{sgn}(\sigma)\mathrm{sgn}(\sigma') \prod_{\substack{j=0 \\ j \neq m,n}}^{N} \langle k|\sigma'_n\rangle_n \langle \sigma_j|\sigma'_j\rangle_j \langle \sigma_m|k'\rangle_m \tag{3.2.27}$$

where $\sigma_{q'}$ was abbreviated by σ' and σ_q by σ. The inner product vanishes unless $\sigma_j = \sigma'_j$ for $j \neq n, m$ and $k = \sigma'_n$ and $k' = \sigma_m$, reducing the double sum in Eq. (3.2.27) to a single one over $(N-1)!$ permutations which each contributes 1. In addition, we require that the $(N+1)$-tuple $\chi = \chi^k_q = \chi^{k'}_{q'}$, where $\chi^k_q = \{k\} \cup \sigma_q$ and $\chi^{k'}_{q'} = \{k'\} \cup \sigma_{q'}$.

Then, we distinguish between two cases. In the first case, we have $k = k' = \sigma_n = \sigma'_m$. Consequently, the two sets σ_q and $\sigma_{q'}$ describe the same selection of N excitation numbers out of possible d. Therefore, we have

$$\langle \pi^{(k)}_{nq} | \pi^{(k')}_{mq'} \rangle = -\frac{1}{N} \delta_{k,k'} \delta_{q,q'}. \tag{3.2.28}$$

In the last case with $k \neq k'$ the two sets σ_q and $\sigma_{q'}$ represent selections of excitation numbers differing by one element. The inner product will be different from *zero* if those elements coincide with the values of k and k', respectively $k = \sigma'_n$ and $k' = \sigma_m$. We have

$$\langle \pi^{(k)}_{nq} | \pi^{(k')}_{mq'} \rangle = (-1)^{|\chi^{-1}(k) - \chi^{-1}(k')|+1} \ \frac{1}{N} \delta_{k,\sigma'_n} \delta_{k',\sigma_m} \tag{3.2.29}$$

where $\chi^{-1}(k)$ and $\chi^{-1}(k')$ denote the position of k and k', respectively, in the strictly increasing $N+1$-tuple χ.

3.2.3 The optimum measurement

In order to maximize P_{succ}, the probability to successfully identify N qudits, we need to find the optimum values of the parameters $\alpha_n^{(k,k')}$. Applying the detection operator Π_n to the state ρ_n we get the probability that the data qudit is in the same state as the n-th reference qudit

$$\begin{aligned} \mathrm{Tr}(\rho_{\mathrm{n}}\Pi_{\mathrm{n}}) &= \sum_{k,k'=0}^{d-1}\sum_{q=1}^{\binom{d}{N}} \alpha_n^{(k,k')}\langle\pi_{nq}^{(k')}|\rho_n|\pi_{nq}^{(k)}\rangle \\ &= \frac{2}{(d+1)d^N}\frac{1}{N!}(N-1)!\sum_{k,k'=0}^{d-1}\alpha_n^{(k,k')}R_{k,k'}^N \end{aligned} \tag{3.2.30}$$

with

$$\begin{aligned} R_{k,k'}^N &= \sum_{q=1}^{\binom{d}{N}}\sum_{\sigma_q}\langle\sigma_{q0}|_0\langle k|_n P_{0,n}^{sym}|k'\rangle_n|\sigma_{q0}\rangle_0 \\ &= \binom{d}{N}\frac{N(d+1)}{2d}\delta_{k,k'}. \end{aligned} \tag{3.2.31}$$

Here it was taken into account that a specific set σ_q does not contain all excitation numbers $\sigma_j = 0, 1, \ldots, d-1$ if $N < d$. On the other hand, if $N = d$ Eq. (3.2.31) reduces to the already known equation [81]

$$R_{k,k'}^d = \frac{(d+1)}{2}\delta_{k,k'}. \tag{3.2.32}$$

The success probability takes the following form

$$\begin{aligned} P_{succ} &= \frac{1}{N}\sum_{n=1}^{N}\mathrm{Tr}(\rho_{\mathrm{n}}\Pi_{\mathrm{n}}) \\ &= \frac{1}{N}\frac{1}{d^{N+1}}\binom{d}{N}\sum_{k=0}^{d-1}\sum_{n=1}^{N}\alpha_n^{(k)} \end{aligned} \tag{3.2.33}$$

where $\alpha_n^{(k)} = \alpha_n^{(k,k)}$. Since the success probability does not depend on non-diagonal elements $\alpha_n^{(k,k')}$ $(k \neq k')$ we put

$$\alpha_n^{(k,k')} = \alpha_n^{(k)}\delta_{k,k'} \tag{3.2.34}$$

Then the constraint for the non-negativity of the detection operators reduces to

$$\sum_{n=1}^{N}\Pi_n = \sum_{k=0}^{d-1}\sum_{q=1}^{\binom{d}{N}}\left(\sum_{n=1}^{N}\alpha_n^{(k)}|\pi_{nq}^{(k)}\rangle\langle\pi_{nq}^{(k}|\right) \leq I. \tag{3.2.35}$$

From Eqs. (3.2.22), (3.2.26) and (3.2.28) follows that the operators in brackets act in orthogonal subspaces for different values of q and different values of k. Therefore, the maximization of the success probability P_{succ} consist of solving $d\binom{d}{N}$ independent maximization problems in orthogonal subspaces belonging to different values of k and different values of q. Hence $\langle\pi_{nq}^{(k)}|\pi_{mq}^{(k)}\rangle$ does not depend on k or q and the indices can be omitted. Then the task of optimizing P_{succ} is equal to maximizing $\sum_{n=1}^{N}\alpha_n \equiv S$ with

$$\sum_{n=1}^{N}\alpha_n|\pi_n\rangle\langle\pi_n| = \Pi_S \leq I \tag{3.2.36}$$

and

$$\langle \pi_n | \pi_n \rangle = 1, \quad \langle \pi_n | \pi_m \rangle = -\frac{1}{N} \quad (m \neq n). \tag{3.2.37}$$

Next, following the same approach as [81], we will make use of the method developed by Chefles and Barnett [51] for optimum unambiguous discrimination of symmetric states. We rewrite the N state vectors $|\pi_n\rangle$ as

$$|\pi_n\rangle = \frac{1}{N}|u_0\rangle + \frac{\sqrt{N+1}}{N} \sum_{l=1}^{N-1} \exp\left(2\pi i \frac{n}{N} l\right) |u_l\rangle, \tag{3.2.38}$$

where the states $\{|u_l\rangle\}$ with $\langle u_l | u'_l \rangle = \delta_{ll'}$ build an orthonormal basis in the N-dimensional subspace spanned by the set of states $\{|\pi_n\rangle\}$. The form of the mutual overlaps given by Eq. (3.2.37) makes it possible to use this representation of the states $|\pi_n\rangle$ and is recovered from

$$\langle \pi_n | \pi_m \rangle = \frac{1}{N^2} + \frac{N+1}{N^2} \sum_{l=1}^{N-1} \left[\exp\left(2\pi i \frac{m-n}{N}\right) \right]^l \tag{3.2.39}$$

using the sum rule for the geometric series. With Eq. (3.2.38) it is easily verified that the states $\{\pi_n\}$ are covariant in respect to the unitary operator $U = \sum_{l=0}^{N-1} \exp\left(2\pi i \frac{l}{N}\right) |u_l\rangle\langle u_l|$ and transform according to $U|\pi_N\rangle = |\pi_1\rangle$ and $U|\pi_n\rangle = |\pi_{n+1}\rangle$ with $n = 1, \ldots, N-1$. It was shown in [51] that then there exists an optimum operator Π_s^{opt} maximizing S that possesses the same symmetry as $|\pi_n\rangle$ in respect to U. Therefore, we have $\alpha_1 = \alpha_2 = \cdots \equiv \alpha$ and the constraint Eq. (3.2.36) takes the form

$$\alpha \sum_{n=1}^{N} |\pi_n\rangle\langle\pi_n| \leq I = \sum_{l=0}^{N-1} |u_l\rangle\langle u_l|. \tag{3.2.40}$$

On the other hand, from Eq. (3.2.38) we obtain

$$\sum_{n=1}^{N} |\pi_n\rangle\langle\pi_n| = \frac{1}{N}|u_0\rangle\langle u_0| + \frac{N-1}{N}\sum_{l=1}^{N-1} |u_l\rangle\langle u_l|, \tag{3.2.41}$$

where the relation$\sum_{n=1}^{N} \exp[2\pi i(l-l')n/N] = N\delta_{(ll'}$ has been taken into account. Inserting Eq. (3.2.41) into Eq. (3.2.40) the largest value of α allowed by the constraint is found to be

$$\alpha^{opt} = \frac{N}{N+1}. \tag{3.2.42}$$

With $\alpha_n^{(k)} = \alpha^{opt}$, Eqs. (3.2.33) and (3.2.23) yield both, the success probability to unambiguously identify N unknown pure qudit states

$$P_{succ}^{opt}(N,d) = \frac{N}{N+1}\frac{1}{d^N}\binom{d}{N} \tag{3.2.43}$$

and the optimum detection operators, with $|\pi_{nq}^{(k)}\rangle$ given by Eq. (3.2.20),

$$\Pi_n^{opt} = \frac{N}{N+1}\sum_{k=0}^{d-1}\sum_{q=1}^{\binom{d}{N}} |\pi_{nq}^{(k)}\rangle\langle\pi_{nq}^{(k}| \quad (n=1,\ldots,N). \tag{3.2.44}$$

The detection operators Π_n^{opt} are not projectors. Therefore, the optimum measurement strategy is a generalized measurement.

Eqs. (3.2.43) and (3.2.44) are generalizations of the results in [81] for d unknown qudit states and [76] for 2 unknown qudit states. This can be seen

if we rewrite the success probability Eq. (3.2.43) as

$$P_{succ}^{opt} = \left\{ \frac{1}{d+1} \frac{1}{d^{d-1}} \right\} \frac{d^d}{d^N} \frac{N}{d} \binom{d+1}{N+1} \tag{3.2.45}$$

where the term in curly brackets represents the result from [81] for identifying d qudit states unambiguously. The remainder of Eq. (3.2.45) denotes the improvement of discriminating in a Hilbert space larger than n_d. This is illustrated in Fig. 3.1.

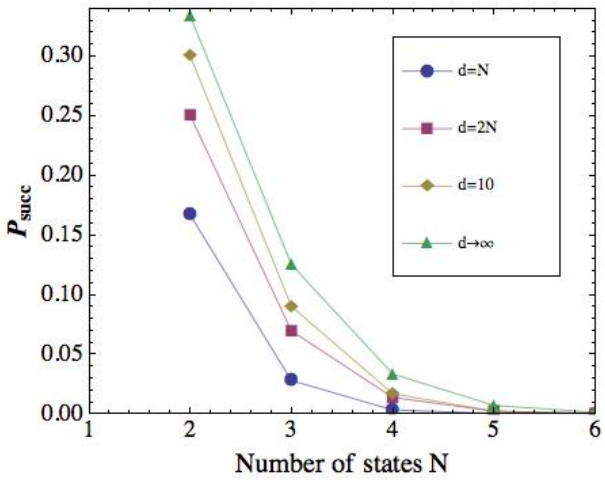

Figure 3.1: The success probability of identifying N unknown states in $d = N$, $d = 2N$, $d = 10$ and $d \to \infty$.

In the case of $N = 2$ states the success probability increases from $1/6$ for $d = N$ to $1/3$ for $d \to \infty$ agreeing with the result from [76]. Furthermore for $N = 3$ states the probability of success increases from $1/36$ for $d = 3$ to $1/8$ for $d \to \infty$.

3.3 Minimum error identification of N unknown pure qudit states

In order to identify the probe qudit with one of the N reference states with minimum error, we have to discriminate between the N density matrices ρ_n given by

$$\rho_n = \frac{2}{(d+1)d^N}\, P_{0,n}^{sym} \bigotimes_{\substack{i=1 \\ i\neq n}}^{N} I_i \qquad (n = 1, \ldots, N) \tag{3.1.4}$$

To perform this task we require N positive detection operators $\Pi_1, \ldots \Pi_N$ whose sum is the identity

$$\sum_{n=1}^{N} \Pi_n = I \equiv I_0 \otimes I_1 \otimes \ldots \otimes I_N. \tag{3.3.1}$$

The detection operators are defined in such a way that $\mathrm{Tr}(\rho_n \Pi_n)$ is the probability of successfully identifying the density operator as ρ_n, while $\mathrm{Tr}(\rho_n \Pi_m)$ $(m \neq n)$ describes the probability to infer an erroneous result.

The optimal detection operators have to satisfy the necessary and sufficient condition [18, 19, 20]

$$\Pi_k \left(\eta_k \rho_k - \eta_j \rho_j\right) \Pi_j = 0 \tag{1.2.10}$$

and

$$\sum_k \Pi_k \eta_k \rho_k - \eta_j \rho_j \geq 0. \tag{1.2.11}$$

Here we are considering that N mixed states occur with equal prior probability, given by $1/N$, so that the overall success probability of the

discrimination measurement takes the form

$$P_{succ} = \frac{1}{N}\sum_{n=1}^{N} \mathrm{Tr}(\rho_{\mathrm{n}}\Pi_{\mathrm{n}}). \tag{3.3.2}$$

This is the quantity we would like to maximize conversely minimizing the error probability.

Due to the symmetry of the density matrices, all ρ_n with $n > 1$ can be expressed in terms of ρ_1 using permutation operators $P_{k,l}$ such that

$$\rho_n = P_{1,n}\rho_1 P_{1,n} \tag{3.3.3}$$

with

$$\begin{aligned} P_{k,l} = I_0 \otimes \sum_{i=0}^{d-1} |i\rangle_k |i\rangle_l \langle i|_k \langle i|_l \\ + \sum_{j=1}^{d-1}\sum_{i=0}^{j-1} (|i\rangle_k |j\rangle_l \langle j|_k \langle i|_l + |j\rangle_k |i\rangle_l \langle i|_k \langle j|_l) \\ \bigotimes_{\substack{i=1 \\ i\neq k, i\neq l}}^{N} I_i \qquad (k,l = 1,\ldots,N \quad \text{and} \quad k \neq l). \end{aligned} \tag{3.3.4}$$

3.3.1 An upper bound

In this section we derive an upper bound that is overly optimistic in that there are no detection operators that can realize it. Let us start by substituting the POVM element that successfully identifies ρ_1 in Eq. (3.3.2) by

$$\Pi_1 = I - \sum_{n=1}^{N} \Pi_n \tag{3.3.5}$$

Then the success probability takes the from

$$P_{succ} = \frac{1}{N} + \frac{1}{N}\sum_{n=2}^{N} \mathrm{Tr}((\rho_n - \rho_1)\Pi_n). \tag{3.3.6}$$

Since, there is nothing special about ρ_1 we replace it by the more general ρ_m, with $n \neq m$, and define the operator $D_{nm} \propto \rho_n - \rho_m$ as

$$D_{nm} = (P_{0,n}^{sym} \otimes I_m - P_{0,m}^{sym} \otimes I_n) \bigotimes_{\substack{i=1 \\ i\neq n,m}}^{N} I_i \tag{3.3.7}$$

leading to

$$P_{succ} \leq \frac{1}{N} + \frac{1}{N(d+1)d^N} \sum_{\substack{n=1 \\ n\neq m}}^{N} \mathrm{Tr}|D_{nm}| \equiv P_{succ}^{bound} \tag{3.3.8}$$

where we made use of the following relation

$$\max_P \mathrm{Tr}(PD) = \frac{1}{2}\mathrm{Tr}|D| \tag{3.3.9}$$

where P is a positive operator $0 \leq P \leq I$ and $\mathrm{Tr}|D|$ is the trace norm with $|D| = \sqrt{D^\dagger D}$. The maximum in Eq. (3.3.9) is attained if and only if P is of the form $P = P_{D_+} + E_{D_0}$. Here P_{D_+} is the projector onto the eigenspace of D with positive eigenvalues and E_{D_0} is any operator in the eigenspace of *zero* eigenvalues of D with $0 \leq E_{D_0} \leq 1$. The equality sign in Eq. (3.3.8) holds provided that the detection operators are of them form

$$\Pi_n = P_+^{(nm)} \quad (n \neq m, n = 1, \ldots N) \tag{3.3.10}$$

where the operators $P_+^{(nm)}$ are the projectors onto the subspace spanned by the eigenvectors of $D_{nm} \propto \rho_n - \rho_m$ belonging to positive eigenvalues. The bound can only be reached if the condition

$$\Pi_m = I - \sum_{\substack{n=1 \\ n \neq m}}^{N} P_+^{(nm)} \geq 0 \tag{3.3.11}$$

is satisfied. This however holds only true for $N = 2$ and not for general N. Hence, the bound in Eq. (3.3.8) is an overly optimistic upper bound. We will see in the next section that the square-root measurement provides a tighter, but lower bound. Therefore, let us follow through with the calculation.

The permutation operator $P_{k,l}$ given by Eq. (3.3.4) exchanges systems k and l. If we apply this operator to D_{nm} with $k = n$ we get

$$D_{lm} = P_{n,l} D_{nm} P_{n,l} \tag{3.3.12}$$

where $l \neq m$. Since $P_{n,l}$ is unitary, $\mathrm{Tr}|D_{lm}| = \mathrm{Tr}|D_{nm}|$ for $l = 1, 2, \ldots N$ and $l \neq m$. Therefore, the sum in Eq. (3.3.8) reduces to $(N-1)\ \mathrm{Tr}|D_{nm}|$ and the upper bound of the maximum success probability takes the form

$$P_{succ}^{bound} = \frac{1}{N} + \frac{N-1}{N(d+1)d^N}\ \mathrm{Tr}|D_{nm}|. \tag{3.3.13}$$

for any fixed values of n and m as long as $n \neq m$.

Now it remains to determine all *non-zero* eigenvalues and their multiplicities of one of the operators D_{nm}. For simplicity we set $n = 1$ and $m = 2$ and omit the subscripts of the operator D. Following the approach of [6] we

first rewrite D in terms of permutation operators

$$D = \frac{1}{2}(P_{0,1} - P_{0,2}). \tag{3.3.14}$$

In order to calculate $\mathrm{Tr}|D|$ we start by computing D^2

$$D^2 = \frac{1}{4}(2 - P_{0,1}P_{0,2} - P_{0,2}P_{0,1}) = \frac{1}{4}(2 - P_{201} - P_{120}) \tag{3.3.15}$$

where P_{201} and P_{120} are permutation operators for the three qudits 0, 1 and 2. Note that the symmetrizer and antisymmetrizer for a system of N particles are given as

$$\mathcal{S} = \frac{1}{N!}\sum_{\alpha} P_\alpha \tag{3.3.16}$$

and

$$\mathcal{A} = \frac{1}{N!}\sum_{\alpha} \epsilon_\alpha P_\alpha \tag{3.3.17}$$

where P_α are $N!$ different permutation operators and $\epsilon_\alpha = 1$ for even and $\epsilon_\alpha = -1$ for odd permutations. Using $\mathcal{S}$ and $\mathcal{A}$ for three qudits Eq. (3.3.15) takes the form

$$D^2 = \frac{3}{4}(1 - \mathcal{S}(012) - \mathcal{A}(012)) = \frac{3}{4}\,\mathcal{M}(012) \tag{3.3.18}$$

where $\mathcal{S}(012)$, $\mathcal{A}(012)$ and $\mathcal{M}(012)$ are the projectors onto the totally symmetric, totally antisymmetric and mixed symmetric subspace of three qudits, respectively.

Then from $|D| = \sqrt{3}/2\ \mathcal{M}(012)$ follows

$$\mathrm{Tr}|D| = \sqrt{3}/2\ d^{N-2} dim(\mathcal{M}(012)). \tag{3.3.19}$$

The factor d^{N-2} arises from the remaining system of $N-2$ qudits represented by identity matrices. The dimension of the mixed symmetric subspace for $d > 2$ can be calculated as

$$\begin{aligned} dim\ \mathcal{M}(012) &= d^3 - \binom{d+3-1}{d-1} - \binom{d}{3} \\ &= \frac{2}{3} d(d^2-1) \end{aligned} \tag{3.3.20}$$

where the dimension of the totally symmetric and the totally antisymmetric subspaces of three qudits are subtracted from the total dimension of the space of three qudits. In the case of qubits there is no totally antisymmetric subspace and the last term in Eq. (3.3.20) can be omitted.

The complete set of eigenvalues of D is 0, $-\frac{\sqrt{3}}{2}$ and $\frac{\sqrt{3}}{2}$ which can be easily tested by working out the qubit case. Substituting Eqs. (3.3.19) and (3.3.20) into Eq. (3.3.13) the maximum success probability of N unknown states in d dimensions is

$$P_{succ}^{bound}(N,d) = \frac{1}{N} + \frac{N-1}{N}\frac{d-1}{d}\frac{\sqrt{3}}{3}. \tag{3.3.21}$$

In the case of $N = 2$ this coincides with the result presented in [6] for the minimum error discrimination of two unknown qudits which is the only case where the bound is reached.

3.3.2 The 'pretty good measurement' and numerical values

Evens so the square root measurement (SRM), also called the 'pretty good measurement', is in general suboptimal it has many desirable properties. The detection operators for SRM are directly constructed from the given set of states and their a priori probabilities. It has been shown that the SRM is almost optimal or 'pretty good' if the states are equally likely and almost orthogonal [95] and in some suboptimal cases it can be made optimal through weighing of some parameters [95, 30, 96]. Furthermore, SRM is in many discrimination problems where the states exhibit certain symmetries the optimal measurement [23, 24, 25, 50, 31, 32]. Therefore, we choose the following form for the detection operators

$$\Pi_n = \rho^{-1/2}\ \rho_n\ \rho^{-1/2} = \rho^{-1/2}\ P_{1,n}\rho_1 P_{1,n}\ \rho^{-1/2} \tag{3.3.22}$$

with $\rho = \sum_n \rho_n$ and $\rho^{-1/2}$ its inverse square root (the inverse taken only over the support of ρ). However, using the necessary and sufficient condition Eq. (1.2.10) we see that these detection operators are not optimal

$$\Pi_k \left(\eta_k\rho_k - \eta_j\rho_j\right)\Pi_j = \tag{3.3.23}$$
$$\tfrac{1}{N}\rho^{-1/2}P_{1,k}\rho_1\rho^{-1/2}\left(\rho_1 P_{1,k}\ \rho^{-1/2}P_{1,j} - P_{1,k}\rho^{-1/2}P_{1,j}\rho_1\right)\rho^{-1/2}\rho_1 P_{1,j}\rho^{-1/2}$$

where we used the fact that ρ is invariant under the transformation $P_{1,k}\rho P_{1,k}$. On the other hand, the permutation operators $P_{k,l}$ do not commute with ρ_n or ρ. Premultiplying ρ_n or ρ with $P_{k,l}$ exchanges the k-th with the l-th row. Postmultiplying ρ_n or ρ with $P_{k,l}$ exchanges the k-th with the l-th column.

Therefore, the SRM is not optimal. However, for the qubit and the qutrit case the values for P_{succ} were calculated for the SRM using Mathematica. The numerical optimization was done with the LMI toolbox in MATLAB using the IQCβ interface from [97]. This is a matrix optimization toolbox based on semidefinite programming. The values are presented together with the upper bound from Section 3.3.1 in Table 3.1 for qubits and in Table 3.2 for qutrits.

N	P_{SRM}	$P_{numerical}$	P_{succ}^{bound}
2	0.644	$0.648 \pm 6.15 \times 10^{-3}$	0.644
3	0.437	$0.447 \pm 4.25 \times 10^{-3}$	0.526
4	0.330	$0.335 \pm 3.15 \times 10^{-3}$	0.467
5	0.265	$0.268 \pm 2.55 \times 10^{-3}$	0.430

Table 3.1: The probability of success for distinguishing with minimum error N unknown qubit states using the SRM, numerical calculations and the upper bound.

N	P_{SRM}	$P_{numerical}$	P_{succ}^{bound}
2	0.692	$0.695 \pm 6.6 \times 10^{-3}$	0.692
3	0.485	$0.496 \pm 4.71 \times 10^{-3}$	0.589

Table 3.2: The probability of success for distinguishing with minimum error N unknown qutrit states using the SRM, numerical calculations and the upper bound.

The success probability from the SRM, P_{SRM}, and the numerically calculated success probability, $P_{numerical}$, are very close to each other while the

overly optimistic upper bound, P_{succ}^{bound}, is obviously too large. Therefore, we conclude that even though the SRM is suboptimal and does not satisfy the necessary and sufficient condition it is a good approximation.

Chapter 4

Summary

The discrimination and identification of quantum states is a non-trivial task for quantum systems with more than two states as well as higher dimensions.

We presented a complete analysis of the unambiguous discrimination of three pure, non-orthogonal states. The problem is characterized by seven parameters, the three overlap amplitudes s_i, the three a priori probabilities η_i and an invariant combination of the phases, the Berry phase ϕ. We started by quantifying the linear independence condition, which is a necessary condition for USD. This condition defines the range of valid values for the overlaps of the states in terms of an invariant, the cocycle ϕ. In general, the range of valid values shrinks if ϕ is increased from 0 to π. This was illustrated by three special cases, first if all amplitudes are equal and second only two of the amplitudes are equal. The third example of the LI condition was in scaled quantities. This was especially illuminating as the positivity constraint in the optimization problem also with scaled quantities had the same exact form. Therefore, the LI condition and the constraint could be

represented by the same graph. With this insight we developed a complete and intuitive geometric picture of the unambiguous discrimination problem. This also led to a classification of the solution in three distinct categories with the worst case scenario that at least one out of the three states can always be discriminated.

Next, we derived the complete solution for the case of vanishing Berry phase $\phi = 0$ and also $\phi = \pi$. We have shown that the optimum measurement is either a single-valued function of the parameters or a bi-valued one, in which case it exhibits a second-order symmetry breaking phase transition-like phenomenon. Furthermore, solutions for arbitrary phase ϕ but either all overlap amplitudes equal or two equal and one different have been presented. In the cases where the weighted equal probably measurement is optimal, it is also tantamount to solutions derived with scaled parameters. The POVM elements in terms of the *a priori* probabilities and the initial states $|\psi_i\rangle$ were derived explicitly. The non- negativity of the POVM for the inconclusive outcome lead to the same constraint as for the USD strategy.

Finally, we point out that the methods for finding the condition for linear independence, the optimum USD strategy and the explicit expression of the POVM as well as the geometric interpretation holds in essence for $N > 3$ states. However, the mathematical complexity of the problem increases with the the number of states and makes exact solutions very impractical. On the other hand, the geometric picture lends itself to a straightforward numerical algorithm for finding the optimal failure probabilities. For $N > 3$ the optimality region is an N-dimensional hyperbolic surface and the $Q =$ *constant* plane is an N-dimensional plane. The common point for the lowest

possible Q is the optimal solution. It can be an internal point or it can be on one of the $N-k$ dimensional borders of the optimality region with $k = 1, \ldots, N-1$. In this latter case precisely $N-k$ states discriminated with finite probability of success, therefore at least one state can always be discriminated.

In addition the identification of N unknown qudit states was investigated. It was shown that, due to our lack of knowledge of the states, this problem is equivalent to discriminating N mixed density matrices. The structure of the detection operators for unambiguous discrimination was explored with the example of three ququarts. The general form was then derived in the following section. Using the positivity of the detection operators the maximum success probability was derived. This reduced to the the already known formula for the unambiguous discrimination of d unknown qudits. For the minimum error identification of N unknown qudits two bounds were derived. The upper bound was termed overly optimistic, since there are no detection operators for $N > 2$ that can satisfy it. On the other hand, the lower bound was found using the conventional description of a square-root measurement. It compared fairly well to the numerical values of the success probability that were calculated using MATLAB. It is therefore possible that a more general approach using a generalized square-root measurement will be optimal.

Furthermore, the success probability increases if there are multiple copies of the data as well as the program states available. This has been explored for the case where the program state is one out of two possible states. For $N > 3$ this is an open problem and remains as a subject for future research.

Bibliography

[1] M. A. Nielsen and I. L. Chuang, Phys. Rev. Lett. **79**, 321 (1997).

[2] M. A. Neumark, Compt. Rend. Acad. Sci. URSS **1943**, 28, 359361.

[3] M. A. Nielsen and I. L. Chuang, *Quantum Computation and Quantum Information* (Cambridge University Press, 2000).

[4] D. Dieks, Phys. Lett. A **92**, 271 (1982).

[5] W. K. Wooters and W. H. Zurek, Nature **299**, 802 (1982).

[6] A. Hayashi,T. Hashimoto and M. Horibe, Phys. Rev. A **72**, 032325 (2005).

[7] M. Sasaki, S. M. Barnett, R. Josza, M. Osaki and O. Hirota, Phys. Rev. A **59**, 3325 (1999).

[8] A. Chefles, S.M. Barnett, J. Mod. Opt. **45**, 1295 (1998).

[9] C. W. Zhang, C. F. Li and G.-C. Guo, Phys. Lett. A **261**, 25 (1999).

[10] H. Sugimoto, T. Hashimoto, M. Horibe and A. Hayashi, Phys. Rev. A **80**, 52322 (2009).

[11] J. Fiurášek and M. Ježek, PRA **67**, 012321 (2003).

[12] Y. C. Eldar, Phys. Rev. A **67**, 042309 (2003).

[13] G. M. D'Ariano, M. F. Sacchi and J. Kahn, Phys. Rev. A **72**, 032310 (2005).

[14] S. Croke, E. Andersson, S. M. Barnett, C. R. Gilson and J. Jeffers, Phys. Rev. Lett. **96**, 70401 (2006).

[15] U. Herzog, Phys. Rev. A **79**, 032323 (2009).

[16] P. Mosley, S. Croke, I. Walmsley and S. Barnett, Phys. Rev. Lett. **97**, 193601 (2006).

[17] S. Croke. P. J. Mosley, S. M. Barnett and I. A. Walmsley, The Europ. Phys. Jour. D **41**, 589 (2007).

[18] C. W. Helstrom, Quantum Detection and Estimation Theory, Academic Press New York (1976).

[19] A. S. Holevo, J. Multivariate Anal. 3, 337 (1973).

[20] H. P. Yuen and R. S. Kennedy and M Lax, IEEE Trans. Inf. Theory **IT-21**, 125 (1975).

[21] U. Herzog, Jour. Optics B **6**, S24 (2004).

[22] K. Hunter, Phys, Rev. A **68**, 012306 (2003).

[23] M. Ban, K. Kurokawa, R. Momose and O. Hirota, Intl. Jour. Theo. Phys. **36**, 1269 (1997).

[24] S. M. Barnett, Phys. Rev. A **64**, 30303 (2001).

[25] E. Andersson, S. M. Barnett, C. Gilson and K. Hunter, Phys. Rev. A **65**, 052308 (2002).

[26] U. Herzog and J. A. Bergou, Phys. Rev. A **65** (R), 050305 (2002).

[27] M. Ježek, Phys. Lett. A **299**, 441 (2002).

[28] J. A. Bergou and U. Herzog, Phys. Rev. A **70**, 022302 (2004).

[29] M. Ježek, J. Řehàček and J. Fiurášek, Phys. Rev. A 65, 60301 (2002).

[30] Y. Eldar and G. Forney, IEEE Trans. Inf. Theo. **47**, 858 (2001).

[31] C. Chou and L.Y. Hsu, Phys. Rev. A **68**, 042305 (2003).

[32] Y. C. Eldar, A. Megretski and G. C. Verghese, IEEE Trans. Inf. Theo. **50**, 1198 (2004).

[33] Y. C. Eldar, A. Megretski and G. C. Verghese, arXiv quant-ph/0211111v1 (2002).

[34] A. Assalini, G. Cariolaro and G. Pierobon, Phys Rev. A **81**, 12315 (2010).

[35] A. Montanaro, Commun.Math.Phys. **273**, 619 (2007).

[36] D. Qiu, Phys. Rev. A **77**, 012328 (2008).

[37] D. Qiu and L. Li, Phys. Rev. A **81**, 042329 (2010).

[38] J. Tyson, Jour. Math. Phys. **50**, 032106 (2009).

[39] S. M. Barnett and E. Riis, J. Mod. Opt. **44**, 1061 (1997).

[40] R. Clarke, V. M. Kendon, A. Chefles, S. M. Barnett, E. Riis and M. Sasaki, Phys. Rev. A **64**, 01203 (2001).

[41] I. D. Ivanovic, Phys. Lett. A **123**, 257 (1987).

[42] D. Dieks, Phys. Lett. A **126**, 303 (1988).

[43] A. Peres, Phys. Lett. A **128**, 19 (1988).

[44] G. Jaeger and A. Shimony, Phys. Lett. A **197**, 83 (1995).

[45] J. A. Bergou, M. Hillery and Y. Sun, Jour. Mod. Opt. **47**, 487 (2000).

[46] A. Chefles, Phys. Lett. A **239**, 339 (1998).

[47] L. M. Duan and G. C. Guo, Phys. Rev. Lett. **80**, 4999 (1998).

[48] C. W. Zhang, C. F. Li and G. C. Guo, Phys. Letts. A, **26**1, 25 (1999).

[49] X. Sun, S. Zhang, Y. Feng and M. Ying, Phys. Rev. A **65**, 044306 (2002).

[50] Y. Eldar, IEEE Trans. Inf. Theory **49**, 446 (2003).

[51] A. Chefles and S. M. Barnett, Phys. Lett. A **250**, 223 (1998).

[52] A. Peres and D. R. Terno, J. Phys. A **31**, 7105 (1998).

[53] Y. Sun, M. Hillery and J. A. Bergou, Phys. Rev. A **64**, 022311 (2001).

[54] M. A. Jafarizadeh, M. Rezaei, N. Karimi and A. R. Amiri, Phys. Rev. A **77**, 042314 (2008).

[55] S. Pang and S. Wu, Phys. Rev. A **80**, 052320 (2009).

[56] L. Roa, C. Hermann-Aviliano, R. Salazar, A. B. Klimov, B. Burgos, O. Jimenez, and A. Delgado, eprint arXiv:quant-ph/0808.0725 (2008).

[57] T. Rudolph, R. W. Spekkens and P. S. Turner, Phys. Rev. A **68**, 010301 (R) (2003)

[58] U. Herzog and J. A. Bergou, Phys. Rev. A **71**, 050301(R) (2005).

[59] U. Herzog, Phys. Rev. A **75**, 052309 (2007).

[60] Y. Sun, J. A. Bergou and M. Hillery, Phys. Rev. A **66**, 32315 (2002).

[61] J. A. Bergou, U. Herzog and M. Hillery, Phys. Rev. A **71**, 042314 (2005).

[62] J. A Bergou, E. Feldman, and M. Hillery, Phys. Rev. A **73**, 032107 (2006).

[63] Feng, R. Duan, and M. Ying, Phys. Rev. A **70**, 012308(2004).

[64] Y. C. Eldar, M. Stojnic, and B. Hassibi, Phys. Rev. A **69**, 062318 (2004).

[65] G. Vidal, L. Masanes and J. Cirac, Phys. Rev. Lett. **88**, 047905 (2002).

[66] M. Hillery, V. Bužek and M. Ziman, Phys. Rev. A **65**, 022301 (2002).

[67] M. Hillery, M. Ziman and V. Bužek, Phys. Rev. A. **66**, 042302 (2002).

[68] M. Hillery, M. Ziman and V. Bužek, Phys. Rev. A **69**, 042311 (2004).

[69] M. Dušek and V. Bužek, Phys. Rev. A **66**, 022112 (2002).

[70] J. Fiurášek and M. Dušek and R. Filip, Phys. Rev. Lett. **89**, 190401 (2002).

[71] J. Fiurášek and M. Dušek, Phys. Rev. A **69**, 032302 (2004).

[72] J. Soubusta, A. Černoch, J. Fiurášek and M. Dušek, PRA 69, 052321 (2004).

[73] J. A. Bergou and M. Hillery, Phys. Rev. Lett. **94**, 160501 (2005).

[74] J. A. Bergou, V. Bužek, E. Feldman, U. Herzog, and M. Hillery, Phys. Rev. A **73**, 062334 (2006).

[75] A. Hayashi, M. Horibe, and T. Hashimoto, Phys. Rev. A **73**, 012328 (2006).

[76] Y. Ishida, T. Hashimoto, M. Horibe and A. Hayashi, Phys. Rev. A **78**, 012309 (2008).

[77] A. Hayashi, M. Horibe, and T. Hashimoto, Phys. Rev. A **72**, 052306 (2005).

[78] B. He and J. Bergou, Phys. Lett. A **359**, 103 (2006).

[79] B. He and J. A. Bergou, Phys. Rev. A **75**, 032316 (2007).

[80] C. Zhang, M. Ying, and B. Qiao, Phys. Rev. A **74**, 042308 (2006).

[81] U. Herzog and J. A. Bergou, Phys. Rev. A **78**, 032320 (2008) and arXiv:0809.4884v2 (2008).

[82] J. A. Bergou and M. Orszag, J. Opt. Soc. Am. **B 24**, 384 (2007).

[83] S. T. Probst-Schendzielorz, A. Wolf, M. Freyberger, I. Jex, B. He, and J. A. Bergou, Phys. Rev. A **75**, 052116 (2007).

[84] B. He and J. Bergou, Phys. Lett. A **356**, 306 (2006).

[85] B. He, J. A. Bergou, and Y. Ren, Phys. Rev. A **76**, 032301 (2007).

[86] B. He, J. Bergou and Z. Wang, Phys. Rev. A **76**, 042326 (2007).

[87] T. Paterek, Phys. Lett. A **367**, 57 (2007).

[88] B. Lanyon, T. Weinhold, N. Langford, J. Obrien, K. Resch, A. Gilchrist and A, White, Phys. Rev. Lett **100**, 060504 (2008).

[89] S. Baek, S. Straupe, A. Shurupov, S. Kulik and Y. Kim, Phys. Rev. A **78**, 042321 (2008).

[90] S. Pancharatnam, Proc. Indian Acad. Sci. A **44**, 247 (1956).

[91] M. V. Berry, Proc. R. Soc. Lond. A **392**, 45-57 (1984).

[92] R. Bhatia, *Positive definite matrices*, Princeton Series in Applied Mathematics (Princeton University Press, 2007).

[93] A. Chefles, Contemp. Phys. **41**, 401 (2000).

[94] J. A Bergou, U. Herzog, and M. Hillery, Lect. Notes Phys. **649**, 417-465 (Springer, Berlin, 2004).

[95] M. Sasaki, K. Kato, M. Izutsu and O. Hirota, Phys. Rev. A **58**, 146 (1998).

[96] C. Mochon, Phys. Rev. A **73**, 032328 (2006).

[97] This software was created by A. Megretski, C-Y. Kao, U. Jönsson and A. Rantzer and is available at http://www.mit.edu/ameg/www/